On optimal pooling of renewable energy sources through risk-averse portfolio optimization methods

by

Chanok Han

A dissertation research proposal submitted to the Graduate Faculty of
Auburn University
in partial fulfillment of the
requirements for the Degree of
Doctor of Philosophy

Auburn, Alabama
May 6, 2022

Keywords: Energy portfolio optimization, Generation forecast error, Intermittency, Energy storage capacity, Multilevel model, Grid system

Approved by

Alexander Vinel, Chair, Associate Professor of Industrial and Systems Engineering
Jorge Valenzuela, Professor of Industrial and Systems Engineering
Kang Bok Lee, Associate Professor of of Information Systems and Business Analytics
Jia Liu, Assistant Professor of Industrial and Systems Engineering

Abstract

This dissertation investigates approaches to achieve optimal pooling of renewable energy sources through risk-averse portfolio optimization methods. The first chapter aims at evaluating the potential for an approach targeted at addressing the issue of limited predictability of wind energy generation, as opposed to intermittency, which has been previously considered in the literature. Specifically, a portfolio optimization model for intelligently constructing a wind energy portfolio for a given harvesting region with the goal of reducing the prediction error is proposed. The mathematical model, based on Conditional Value-at-Risk (CVaR) optimization methodology, is used to evaluate potential improvement in (day ahead) generation predictability for a collection of locations in the USA. The study concludes that pooling indeed can significantly reduce wind energy generation forecasting error, with the effect largely dependent on the size of the harvesting region. Further, if advanced optimization techniques are used, it is possible to balance this reduction with average generation output.

The second chapter aims to evaluate the impact of reducing limited predictability on battery sizing through creating a 'proof-of-concept' experiment. In particular, a heuristic approach is proposed to the problem of simultaneous optimization of generation portfolio and battery sizing. The mathematical models is a bi-level problem, based on conditional risk value (CVaR) optimization methodology on the first level, and a operational planning problem to evaluate installed battery capacity on the second. The study concludes that the heuristic approach with pooling significantly reduces required battery capacity according to operational plans, and the effect varies on the size of the harvesting region or the degree of the technology combination. Further, it is possible to diversify the pooling leading to overall operational cost reduction. Consequently, the results imply that the positive effect of pooling diverse wind resources can be an important factor in planning for generation expansion projects.

Lastly, the third chapter considers a similar multilevel modeling approach, but solves it exactly. The mathematical model is used to evaluate potential cost improvement in a Virtual Power Plant (VPP). In particular, at the first level, Mean conditional risk value (Mean-CVaR) optimization model is used to create an optimal portfolio for minimizing intermittency. The second level of the optimization procedure is based on linear programming for operation planning to minimize the total operation cost. The bi-level problem is solved by employing optimality conditions. The study shows that the multilevel model leads to significant savings in total operation cost compared to the benchmark (heuristic methodology). Further, the total cost is also significantly decreased as the pooling region is increased. This improvement is directly related to the size of the harvesting region. Consequently, this research contributes to the operational planning in VPPs through a multilevel model that advanced pooling approaches.

Acknowledgments

First, and most of all, I am deeply grateful to my advisor Dr. Alexander Vinel for his encouragement and advice during the Ph.D. program at Auburn University. His professional feedback on my research, academic expertise and mentorship made it possible to complete my journey to Ph.D.

I thank Dr. Jorge Valenzuela, Dr. Kangbok Lee, and Dr. Jia Liu for serving on my dissertation committee. The instruction and feedback that I received were invaluable. Also, I am thankful to Dr. Han for reviewing my dissertation as a university reader.

I would like to thank the friends I have made during the Ph.D. program: Dr. Erin Garcia, Dr. LuAnn Carpenter, Dr. Hyuncheol Baik. As a military officer who has been supported by the Republic of Korean Army, I would like to thank the government of the Republic of Korea. Also, I deeply appreciate my senior officer Col. Han (Dr.) for his warm encouragement as a mentor. I would like to thank the friends I have made during the Ph.D. program. Particularly, a special thanks to an old friend of mine, Dr. Dongjin Cho, and Dr. Jinho Jung.

I'd like to thank my father and grandmother for their endless love and encouragement in the sky. Also, I'd like to thank my two big sisters, father-in-law, mother-in-law, and relatives for their support. Most importantly, special thanks to my beloved wife - Hyeran, and lovely daughters - Jimin - for their dedicated love and support throughout my life. None of this would have been possible without you all. Moreover, I give mother all my glory and thanks. I love you from the bottom of my heart. Finally, I thank the Buddha for teaching me to be humble and dedicated.

I will start a new voyage of my life with the people I am grateful for and the good memories in my heart. I can do it, as always.

Table of Contents

List of Figures

List of Tables

Chapter 1

Introduction

Generation output variability is often cited as a significant drawback of many renewable energy sources, particularly, wind and solar [1]. Two facets of variability that are often considered are intermittency and (limited) predictability. Intermittency usually refers to the extent to which a power source is unintentionally stopped or partially unavailable (due to the underlying weather factors in the case of wind and solar power). Predictability refers to the ability of the operator to accurately estimate ahead of time the amount of electricity that can be generated in the future. By definition, an energy source can be intermittent but predictable, or vice versa. In the case of wind energy, both issues can be significant factors. The amount of electricity produced at any given point in time by a given wind plant will depend on wind speeds and air density both of which can rapidly change, resulting in intermittency [2]. Both, while variable, can be highly predictable in the short term. At the same time, over longer periods, e.g., a day ahead, wind speed forecasting, in particular, can be poor [3]. While employing portfolio-based approach for reducing renewables' intermittency has been studied in the literature, similar effect on forecasting error has not been widely explored. Consequently, the first research direction, considered in this dissertation considers modern portfolio optimization techniques as a way to address this gap.

Renewable energy is a valuable supplement or even (in the near future) a replacement to conventional energy sources fuelled by growing concerns about the environmental impacts of the electricity sector. There has been an increasing interest to invest in renewable energy. For example, 60.4 GW of wind energy capacity was installed globally in 2019, a 19% increase from installations in 2018, the second-best year for wind historically ([4]). At the same time, the maximum penetration of renewable energy is limited by the variability nature of the energy input. Moreover, it is important to note that both this effect and generation potential are dependant on characteristics of the region. As a result, the grid system needs to prepare more ancillary services and build infrastructure, such as energy storage systems to address the issue of variability. Therefore, it is important for policymakers to be aware of the best strategies for efficient installation of such ancillary services and for building energy storage systems since the associated cost may not be trivial ([5]). The size of an ESS is one of the most important factors, which can be even more important for microgrids since the cost of batteries may constitute a sizable portion of the overall investment in this case. Therefore, downsizing an energy storage system is desirable. To this end, we secondly propose a heuristic approach for accounting for the presence of storage capacity and demand, and investigate to which extent pooling can be helpful in this case. We specifically concentrate on the question of whether pooling from geographically large areas may be beneficial. Note that even if the customer is not distributed over a large area, it may still be possible to take advantage of geographical pooling. For instance, the TransWest Project in the United States seeks to build a new grid infrastructure to balance renewable energy by supplying renewable energy produced in Wyoming to the southwest [6].

Virtual power plants (VPPs) are a special type of agent, that is particularly suitable for taking advantage of pooling, as investigated here. VPPs integrate a number of distributed energy resources in different areas and, aim to exhibit coordinated dispatching through the networks of distributed energy resources and energy management system (EMS) ([7]). They can be relatively flexible in constructing the energy portfolios and so can more easily take advantage of optimization techniques ([8]). At the same time, the importance of renewable energy within the smart grid is increasing due to the problems caused by the excessive use of fossil fuels ([9]). For example, European Union (EU) has a goal to achieve zero net emissions of greenhouse gases for all EU member states by 2050, in response to climate change process ([10]). However, renewable power uncertainty (intermittency) is still recognized as a disadvantage. Even in the case of wind energy, the volatility of production is high depending on climate conditions (wind speed, air density), etc. Indeed, high intermittency results in requirement to increase either the installed wind facility or backup generations in order to be able to meet demand. To mitigate high intermittency, it is widely accepted that by combining together resources from varied geographical locations it is possible to reduce the severity of issues related to intermittency [11]. Hence, it is clear that aiming to diversify the portfolio of renewable energy reduces the uncertainty in the energy management system. Apart from renewable power uncertainty, load demand and market price are also common uncertainties in VPPs optimization problems. On the other hand, VPPs can explicitly optimize the generation portfolio, since they are not restricted by capital investment constraints. Consequently, the final chapter of this research effort investigates the effect of simultaneous optimisation of generation portfolio, storage investment and operational performance, resulting in combined optimization problem. While the previous chapter, this problem was solved heuristically (by splitting the stages), in the final chapter we find exact optimal solution by employing optimality conditions.

The contributions of the modeling approach from the optimization perceptive are as follows. In the first topic, we develop an optimization framework for designing wind energy portfolios for reducing forecasting error based on the mean-CVaR portfolio design problem that minimizes the risk associated with forecasting error, while ensuring satisfactory average performance. The problem is formulated as an LP and follows from the usual risk-averse stochastic optimization framework. In the next topic, we proposed a two stage optimization problem, where on the first stage the generation portfolio is selected, and then on the second stage, an ESS sizing problem is solved. Due to computational challenges, we also investigate a heuristic approach to solving it, whereby the stages are separated and solved one after the other. In the last topic, we design a multilevel model optimization problem for optimizing a wind energy portfolio and optimization of operation planning at the same time, this time solved exactly. This approach is more comprehensive compared to the two-stage model by allowing to optimization of the total cost over both operation planning and portfolio simultaneously, by employing optimality conditions for the lower-level problem.

The remainder of the dissertation is organized as follows. Chapter 2 provides a research result of Reducing forecasting error by optimally pooling wind energy generation sources through portfolio optimization. Chapter 3 presents the research result of optimizing the energy storage capacity through portfolio optimization in a smart grid system. Chapter 4 discusses the research result of the Multilevel modeling with a risk-averse model for renewable energy management in virtual power plants. Finally, the conclusion part concludes the discussion, limitation and outlines some ideas for future research.

Chapter 2

Reducing forecasting error by optimally pooling wind energy generation sources through portfolio optimization

2.1 Introduction

It is widely accepted that reduction of variability can have a direct benefit to competitiveness of renewable energy. Naturally, high intermittency results in the need to increase either the installed renewable energy capacity or backup conventional generation in order to be able to satisfy demand during the periods of low renewable generation. Similarly, an increase in generation predictability can significantly simplify and/or increase efficiency of planning and operation of the energy grid, for example in the case unit commitment problems, which often rely on day-ahead generation forecasts and are often formulated as stochastic programs. Note though that variability of an energy source can have smaller effect on the overall system if either renewable sources penetration is low, or ample storage is available. At the same time the former condition is not desirable due to the environmental considerations, while the latter can require prohibitively expensive investment levels. Even if relatively large-scale storage is feasible, it is still beneficial to reduce source variability, since it can result in improved overall system efficiency. This then means that, if possible, significant reduction in variability has the potential to make renewable energy more competitive, and hence, enable its wider use.

It is well-established in the literature that by combining together resources from varied geographical locations and/or technologies it is possible to reduce severity of issues related to intermittency. This can be easily understood by noting that any time two uncorrelated (as well as poorly or negatively correlated) signals are combined, the overall variance is reduced, resulting in a phenomenon often referred to as risk reduction through diversification. While the weather (wind speed or solar irradiation) changes very little over a small area, it can vary significantly over larger regions, making it possible to take advantage of diversification. Multiple researchers have pointed out ways to exploit this effect and outlined potential benefits. For example, [12] noted that: "high frequency variability of wind-generated power can be significantly reduced by coupling outputs from 5 to 10 wind farms distributed uniformly over a ten state region of the Central US. More than 95% of the remaining variability of the coupled system is concentrated at time scales longer than a day, allowing operators to take advantage of multi-day weather forecasts in scheduling projected contributions from wind". More examples and some conclusions are reviewed in Section 2.2.

This work focuses on two issues related to geographically pooling renewable energy sources (wind generation in this case), that are not widely studied in the literature. First, the same mechanism that results in reduction in intermittency with geographical pooling also applies to forecasting error. Indeed, it is natural to expect that the difference between the actual and predicted wind generation will be strongly correlated over smaller regions and only weakly correlated over the larger ones. Hence, it is surmised that it may be possible to simultaneously reduce severity of both intermittency and unpredictability of renewable generation. At the same time, this aspect of the effect of geographical pooling of generation sources has not received as much attention. Secondly, most of the existing research claiming benefits due to pooling does not focus on the best strategies for such pooling. In other words, most of these results are based on simple, often naive, approaches to designing geographically diverse energy portfolios (usually, by simply combining equally sized production sites). At the same time, it is also clear that by applying more advanced diversification tools it may be possible to further improve on pooling benefits. For example, the covariance structure between geographically diverse generation sites (and corresponding forecasts) may be complicated with some pairs of generation profiles less correlated than others, which can be exploited through intelligent overarching planning.

Consequently, the goal of this effort is to consider the following three research questions:

1. to what extent is it possible to reduce the forecasting error in wind energy generation by pooling together geographically diverse sources;

2. how much is such pooling efficiency dependent on considering advanced portfolio optimization techniques;

3. how large of an area is required in order to take advantage of improved forecasting accuracy due to pooling.

To this end, we design a simulation study, based on realized and foretasted (day ahead) wind generation data for a collection of states in the US. This paper uses risk-reward portfolio optimization with Conditional-Value-at-Risk (CVaR) as the underlying pooling technique due to its popularity in stochastic optimization research. One year worth of historical observations (training data) is used to construct a collection of optimized wind generation portfolios as well as benchmark options, and then evaluate their performance in terms of average generation and forecasting error for a series of test regions, ranging from county-level to state-level.

The contributions of the effort are as follows. First, this paper develops an optimization framework for designing wind energy portfolio with the goal of reducing forecasting error based on mean-CVaR portfolio design problem, i.e., a problem that minimizes the risk associated with forecasting error (measured by CVaR), while ensuring satisfactory average performance. Secondly, by employing the model in a case study, it can be observed that the forecasting error in wind generation on a state-level can be significantly reduced for all six states tested, with the scale of this improvement dependent on the size of the harvesting area. We observe that, while it is possible to reduce forecasting error by straightforward approaches without portfolio optimization, employing advanced analytical approach allows for careful balancing of average generation and forecasting error. Furthermore, significant reduction in error can be observed with relatively few generation locations pooled. The study also quantifies the effect of distance on pooling efficiency, which varies from 1% to 4% reduction in relative forecasting error per 100km of diameter. Finally, we also illustrate how the proposed portfolio can lead to an increase in use of renewables by considering a battery sizing problem. Specifically, for the example instance considered, the pooled sources allow for a significantly higher proportion of energy from renewable used compared to non-pooled portfolios.

The proposed model and the conclusions can be used in a number of settings related to planning of renewable energy expansion. Virtual power plant (VPP) design and operation can be an example particularly suitable for such analysis. VPPs are service providers acting as an intermediary between distributed energy sources and the wholesale power market. As such, they can be relatively flexible in constructing the energy portfolios and so can more easily take advantage of optimization techniques. See [8] for a detailed discussion of VPPs, their role in energy markets and their effect on integration of renewables.

This research also has a direct relevance to the very broad set of research topics related to design of electricity markets in the presence of large proportion of renewable generation and coalition building in smart grids, see for example, [13, 14] among many others. While these are not directly discussed here, since the considered modeling approach by design relaxes many practical considerations in order to specifically consider the effect of pooling on forecasting error only, the conclusions made can be relevant in informing the potential benefits of expanding geographical diversity of renewable generation sites.

The remainder of the paper is organized as follows. Section 2.2 provides a review of relevant literature. Section 2.3 presents the proposed risk-averse optimization model with mathematical formulation and the corresponding methodology used to organize the case study. Section 2.4 discusses the results of the case study. Finally, Section 2.5 concludes the discussion and outlines some ideas for future research.

2.2 Literature Review

The idea of reducing generation output variability through pooling intermittent energy sources together is not novel and has been widely accepted in the literature. A number of approaches looking to describe this effect from different perspectives have been proposed so far and a thorough review of some of these can be found in [15]. Since most of the relevant literature deals with intermittency aspect of renewables variability, we first briefly review results related to the effect of pooling geographically or technologically diverse generation sources for smoothing the output profile. We then move on to reviewing the limited literature on wind energy forecasting as related to variability reduction. We also briefly discuss the problem of wind generation forecasting itself. We conclude with an overview of (stochastic) optimization methods that have been applied to renewable energy portfolio design.

Reducing intermittency through pooling The underlying principle of risk reduction through diversification relies on the possibility of combining weakly correlated (or negatively correlated) output signals together. A number of studies have presented evidence of weak negative correlation between wind and solar generation profiles for a wide variety of countries and climates. For example, [16] found that solar and wind power are negatively correlated on all time scales, from hourly to annual, but that the correlation is strongest for monthly totals in Sweden. Other examples can be found in [17, 18]. Similarly, even in the absence of technological diversity, i.e., if, for example, only wind energy sources are considered, very weak output correlations can be observed as long as harvesting area is large enough, as observed in, among others, [19] and [20]. The authors of [21] found an 87% reduction of the variability of a single wind plant is obtained by interconnecting 4 wind plants located over 500 km apart. Consequently, we can conclude that there exists clear evidence that larger harvesting areas can contain locations with diverse generation profiles, which, if combined into portfolios, may lead to reduction of variability.

A number of studies have attempted to evaluate the effect of such reduction under specific practical applications. This can be achieved by considering either a practical power systems setting or applied investment problem. Examples of the former include [22], which proposed a risk-averse model with technical power constraints for an energy portfolio; and [23], in which the authors studied the integration of RES into a distribution network with power system constraints to optimize the framework. A typical example of the latter case is [24], which considers the problem of constructing a virtual power plant by pooling different real solar and wind plants together. In [25], the authors proposed an economic model for minimizing investment risk and maximizing the internal rate of return (IRR) of a portfolio of renewable in the Spanish electricity market. The research in [26] presents an investment timing and capacity selection plan based on Real Options analysis for renewable energy assets. The authors of [27] quantified the geographic smoothing effect of large-scale wind energy deployment (1300 wind farms) over various spatial and temporal scales using a variance minimizing algorithm. Finally, [28] presented Monte Carlo simulations model for the benefits of geographic diversity of wind generation and investigated upper bounds on the degree of achievable smoothing according to the number of plants and on the size of the geographic area.

Wind generation forecasting and pooling Predictability problem is distinguished from intermittency (variability) and both are closely related to decision-making in operations and markets [29]. Majority of the existing studies described above explicitly focus on exploiting reduction in intermittency (i.e., smoothing of energy generation). At the same time, as already noted, it is natural to surmise that similar approaches can be viable for the purpose of reducing forecasting error. Indeed, a number of studies have investigated the correlation structure between solar and wind or between a collection of wind or solar sources, which generally confirm existence of weak negative correlations between wind and solar error, as well as weak correlation in forecasting error of geographically distant wind outputs. For example, [30] found that the smallest forecast error is obtained by combining 30% solar and 70% wind resources for Brazil's Northeast region.

Note that the problem of wind (or solar) energy generation output prediction is in itself very challenging and, depending on the forecasting approach, pooling may result in different outcomes. Most efforts focused on either a physical or statistical modeling using meteorological data to improve the accuracy of generation forecast [31]. For example, [32] proposed artificial neural network (ANN) model for a short term wind power generation forecast, while [5] focused on meteorological aspects (solar irradiance, wind speed, etc.) to improve an artificial neural network (ANN) model. Other examples of such an approach can be found in [33, 34]. For our purposes, this study uses already generated forecasted wind generation data openly available through the National Renewable Energy Laboratory (NREL) [35]. It uses the Weather Research and Forecasting Model (WRF) run on a 2-km grid over the continental United States at a 5-min resolution. A detailed description of the underlying models is available in [36, 37].

It is worth emphasizing that many of the studies cited above that are explicitly looking at the effect of pooling do not in fact employ any advanced risk optimization methodology and instead rely on naive diversification. Advanced stochastic optimization models have been used in a number of similar settings and are usually focusing on capital planning, operation cost minimization, plant profit maximization, etc. Some of these studies are reviewed in the remainder of this section.

Optimization methods for renewables portfolio design From the optimization methodology perspective, most approaches widely used in financial portfolio design have also been used in energy portfolios, e.g., Markowitz mean-variance, real options analysis, Internal Rate of Return (IRR), Value-at-Risk (VaR), and Conditional-Value-at-Risk. For example, [38] studied risk analysis for the solar and wind financial planning of investment cost by implementing VaR and Expected VaR in the simulations conducted. This methodology was also applied in [39] to evaluate proposed roadmaps for solar PV and wind-onshore energy. The research presented here employs mean-CVaR optimization methodology, and consequently in the remainder of this section we focus on CVaR optimization models.

Originally proposed for financial portfolio optimization in [40, 41], CVaR is a measure of risk that represents the average losses over a number of worst cases. Naturally, it can be used to limit the risk and is often considered as the standard approach in many stochastic optimization applications, including energy portfolio design. CVaR, by definition, can be used to assess the effect of the tail of the loss distribution, and so is particularly relevant for the applications involving heavy-tailed distributions. In the case of energy planning, these often include wind and/or solar generation, market prices and energy demand, or more long term risks, such as effect of climate change or policy decisions. Further, as is the case with financial applications, risk-aware decision making can be important on different time scales, as long as the underlying process can be sensitive to sudden changes in the stochastic parameters.

In the case of a long-term planning horizon, capital planning problems are often considered. For example, the authors of [42] combined real options analysis and CVaR portfolio optimization theory to assist investors with capacity planning in power generation assets under uncertain climate policy, while [43] suggested a CVaR model to evaluate the risk-reward characteristics in U.S. listed infrastructure index returns. Research efforts that can be characterized as medium-term planning include, among others, [44], which developed a generation company model that applies market price forecasts to the risk-constrained stochastic price-based unit commitment (PBUC) in energy and ancillary services markets, as well as [45], which proposed a stochastic mixed-integer linear model for maximizing the joint profit of wind and hydro units.

CVaR has also been employed in addressing uncertainty related to immediate volatility of either renewable energy generation or market electricity prices. To list a few notable examples, the authors of [46] studied a CVaR model for identifying bidding strategies in short-term energy markets for a wind power producer that enable a significant decrease in the risk of profit variability for a comparatively small reduction in expected profit. In [47], the authors proposed a risk averse scheduling model for the next 24 hours with a minimum CVaR objective for maximum operation revenue. The authors of [48] developed a CVaR-based algorithm for two different short-term (a time horizon of 1 week) problems, where the decision-makers are exposed to high volatility of electricity spot market price. Other similar examples of such a short-term approach can be found in [49] and [50].

A comprehensive review of advantages and disadvantages of different risk-averse approaches to decision making under uncertainty from the perspective of stochastic optimization can be found in [51]. Primarily following the discussion there, we chose to use CVaR as the basis for the optimization problem in this effort for the following reasons. First, as evidenced by the review above, it has been extensively used in decision making related to electricity generation before, including in similar circumstances. Secondly, when employed in an optimization framework (as is the case in this study), it allows for an efficient implementation as a linear program. It must be emphasized that some other approaches, e.g., VaR, chance constraints or variance-based analysis, can lead to significantly more challenging formulations from the numerical perspective, while the use of CVaR allows us to solve relatively large-scale instances (1 year worth of hourly generation scenarios). Finally, CVaR is a coherent measure of risk and has been shown to conform to a number of intuitive requirements for a decision making under uncertainty criterion.

The approach used in the current research effort is most similar to the models presented in [24] and [15]. The former, considers an energy portfolio optimization problem for virtual power plant with the goal of reducing the risk due to volatile wind and solar generation and constructs stochastic scenarios based on hourly records. In contrast, here we focus on quantifying the effect of pooling rather than operational planning. The latter, also employs hourly wind and solar generation volatility to illustrate the ability of portfolio optimization techniques to reduce renewable energy intermittency. The research presented here employs a similar framework but focuses on effect of pooling on forecasting error.

2.3 Research methodology

The study is organized as a series of simulation experiments. A collection of diverse geographical areas (from county to state-sized) is selected for the analysis. For each region, this study chooses a subset of wind generation sites available through NREL [35]. We then apply the procedure depicted in Figure 2.1. We first download historical data on hourly wind energy generation and (hourly) day-ahead forecast for the selected collection of sites. Years 2008–2012 were selected for the analysis based on data availability. After data pre-processing, a portfolio optimization tool (mean-CVaR) is applied to obtain a family of optimal generation portfolios with the goal of minimizing the forecasting error over training period of one year (2008). We then compare their performance (over the testing period of 2009–2012) against benchmark approaches.

It is worth noting here that, while the total of five years worth of data is available, in the remainder of this manuscript only the first year is used for training (solving the optimization problem) and the rest for testing (evaluating portfolio generation profile). First, naturally, one year worth of data is the minimum duration that is still able to account for seasonality, which coupled with the need to reduce the size of the testing set for the sake of computational efficiency is the primary reason for this choice. Secondly, in a preliminary analysis it was established that optimal portfolios obtained based on more than one year of training data do not significantly differ from the base case used here, which was not the case for training sets smaller than one year. We do not report on these results in detail here for the sake of brevity.

2.3.1 Data sources description

We collected actual and forecast generation data provided by National Renewable Energy Laboratory (NREL) from DR POWER [35]. The database provides observations on actual and forecasted wind energy generation for wind sites installed in the U.S. Specifically, the data is derived from the Wind Integration National Dataset (WIND) Toolkit [52]. Meteorological data is

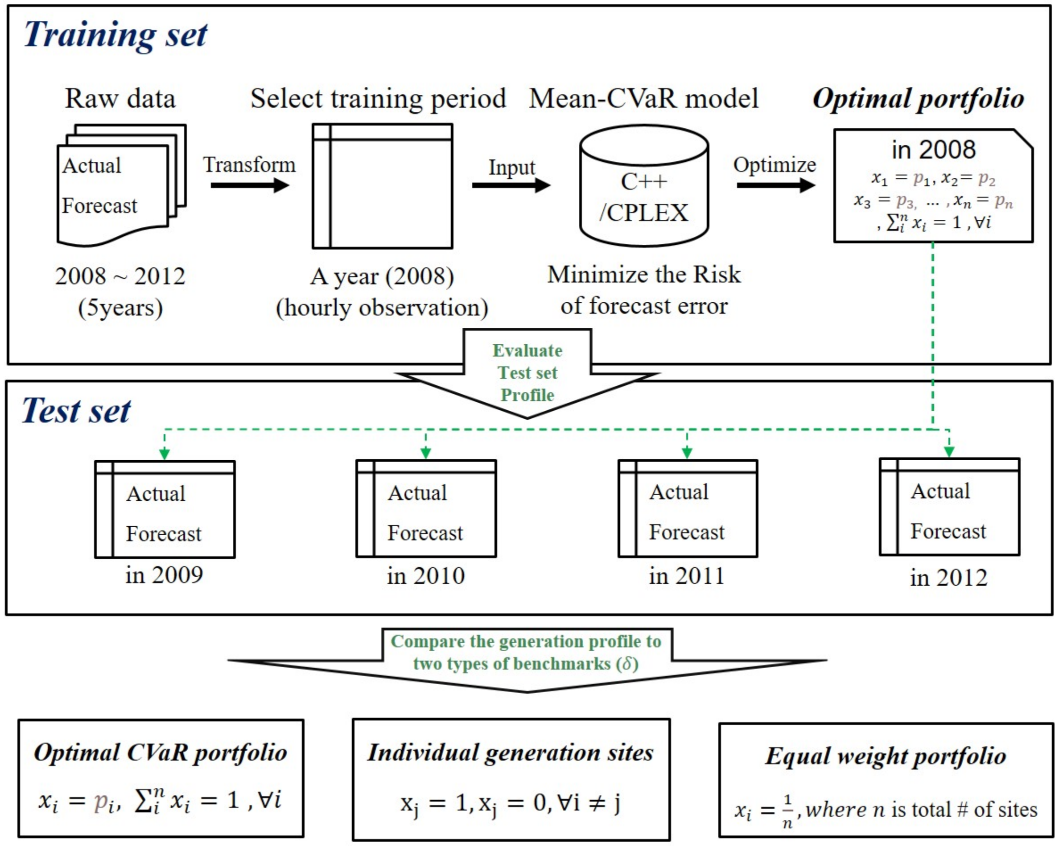

Figure 2.1: Diagram of the overall case study framework.

reported for measurements at 100m above ground level at 5-minute resolution and supplemented with computed wind power (MW/h) assuming a 100m standard hub height. Forecast wind generation data is generated as hour or day ahead. For our case study, we only use the calculated wind generation values down-sampled to hourly observations (to match with the forecast data) and day-ahead forecast. Finally, we scale the generation and forecasted values by applying Levelized Cost of Electricity (LCOE) as a normalization parameter, since it is a commonly used in renewable energy studies [53, 54, 55]. Note that for our purposes here scaling is, in fact not important, since the CVaR minimization problem is scale-independent.

2.3.2 Modeling assumptions

The proposed portfolio design model makes the following important simplifying assumptions.

- We concentrate on wind generation only. Note that a similar study could be conducted for solar energy. We do not include solar in the current study since no similar forecasted data has been available to the authors with sufficient time and spacial resolution.

- We assume that portfolio selection problem consists of two decisions: selection of generation sites and their corresponding investment levels. Further, investment in each location is independent from the rest of the system (only bounded by the overall budget).

- Generation observed from each site is linearly proportional to the investment level. In other words, any discrete or nonlinear dependency between investment and generation capacity are ignored.

- Considerations related to storage and transmission costs are also ignored. Note that in practice pooling efforts are closely related to expansion of the transmission system and energy storage infrastructure. However, to avoid confounding the pooling effects with transmission or energy storage effects, we purposely eliminate the power engineering constraints in this paper.

These assumptions, while making the model less practical, allow us to construct computationally tractable mathematical model, and hence, evaluate the potential effect of pooling on wind energy generation and forecasting error, as detailed with the research questions identified above.

2.3.3 Data sources description

Actual and forecast generation data is available through National Renewable Energy Laboratory (NREL) and DR POWER database [35]. It provides observations on actual and forecasted wind energy generation for wind sites installed in the U.S. Specifically, the data is derived from the Wind Integration National Dataset (WIND) Toolkit [52]. Meteorological data is reported for measurements at 100m above ground level at 5-minute resolution and supplemented with computed wind power (MW/h) assuming a 100m standard hub height. For our case study only the calculated wind generation values down-sampled to hourly observations are used to match with the forecast data which is only available with hourly resolution. Note that while both hour-ahead or day-ahead forecasts are provided (both with hourly resolution), only the day-ahead series are employed for the case study. It can be expected that hour-ahead forecasts are relatively accurate, which naturally severely bounds the potential effect of pooling on reducing that particular error. Further, day-ahead forecasts are widely used in planning, for example, unit commitment problems [56].

2.3.4 Risk-averse optimization model

Our portfolio construction methodology is based on risk-averse stochastic optimization, mean-Conditional Value-at-Risk (mean-CVaR). A detailed review of risk-averse stochastic optimization literature is beyond the scope of this discussion. The reader is advised to consider [40, 41] for a discussion of CVaR, as well as [51] for a comprehensive survey of risk optimization methods. Approach similar to ours has been previously considered in [15]. Note though, that there the model is used for balancing intermittency in energy generation (by minimizing CVaR of the observed energy output). Since the goal here is in minimizing the forecasting error, the model should be amended accordingly. Specifically, the constructed optimization problem minimizes the CVaR of relative forecasting error over the training set, which, by design can translate into more favorable error profile over the testing set.

Consider the problem of constructing the optimal energy portfolio, by pooling n pre-identified potential generation sites. Denote as $\mathbf{A}$ and $\mathbf{F}$ random vectors representing the actual and (day-ahead) forecasted generation from the selected sites. These can be modeled as taking values according to one of equiprobable scenarios based on historical observations, i.e., A_{ij} and F_{ij} give the actual and forecasted generation at site i under scenario j, where j corresponds to all hour-long periods in the training set (total of m records).

The problem is then to select portfolio weights x_i for each site i, so that the obtained generation profile exhibits desired properties. Specifically, in a mean-CVaR framework, the portfolio such that it guarantees a level of average generation and minimizes the risk of forecasting error (measured by its CVaR) is selected. In this case, the average generation from portfolio $\mathbf{x}$ can be evaluated as $\sum_i^n \bar{A}_i x_i$, where $\bar{A}_i$ is the average generation at site i. Forecasting error (random vector $\varepsilon(\mathbf{x})$) under scenario j is given by $\varepsilon_j = \left| \sum_{i=1}^n (A_{ij} - F_{ij}) x_i \right|$. Then define the problem of minimizing the CVaR of the forecasting error, while maintaining target average generation as

$$\min_{\mathbf{x}\in\mathbb{R}^n} \left\{ \text{CVaR}\Big(\varepsilon(\mathbf{x})\Big) \;\middle|\; \sum_i^n x_i = 1,\ \mathsf{E}(\mathbf{A}^\mathsf{T}\mathbf{x}) \geq A_0,\ \mathbf{x} \geq 0 \right\}, \tag{2.1}$$

where A_0 denotes the target average generation and α gives the tail parameter in CVaR. Using standard optimization problem formulation for CVaR (see more details in [51]) it can be reformulated as the following linear program, by introducing auxiliary variables $\mathbf{w}$ and η.

$$\min_{\eta\in\mathbb{R},\mathbf{w}\in\mathbb{R}^m,\mathbf{x}\in\mathbb{R}^n} \quad \eta + \frac{1}{(1-\alpha)m} \sum_j^m w_j \tag{2.2}$$

$$\sum_i^n x_i = 1 \tag{2.3}$$

$$\sum_i^n \bar{A}_i x_i \geq A_0 \tag{2.4}$$

$$w_j \geq -\left| \sum_{i=1}^n (A_{ij} - F_{ij}) x_i \right| - \eta \tag{2.5}$$

$$\mathbf{x}, \mathbf{w} \geq 0. \tag{2.6}$$

The problem is a linear program, which can be solved with standard optimization approaches. The solutions obtained for a collection of values of α and A_0 then give a family of optimal portfolios.

Varying A_0 balances the trade-off between the average generation and forecasting error, while α is a technical parameter responsible for defining risk tolerance.

2.3.5 Case study procedure

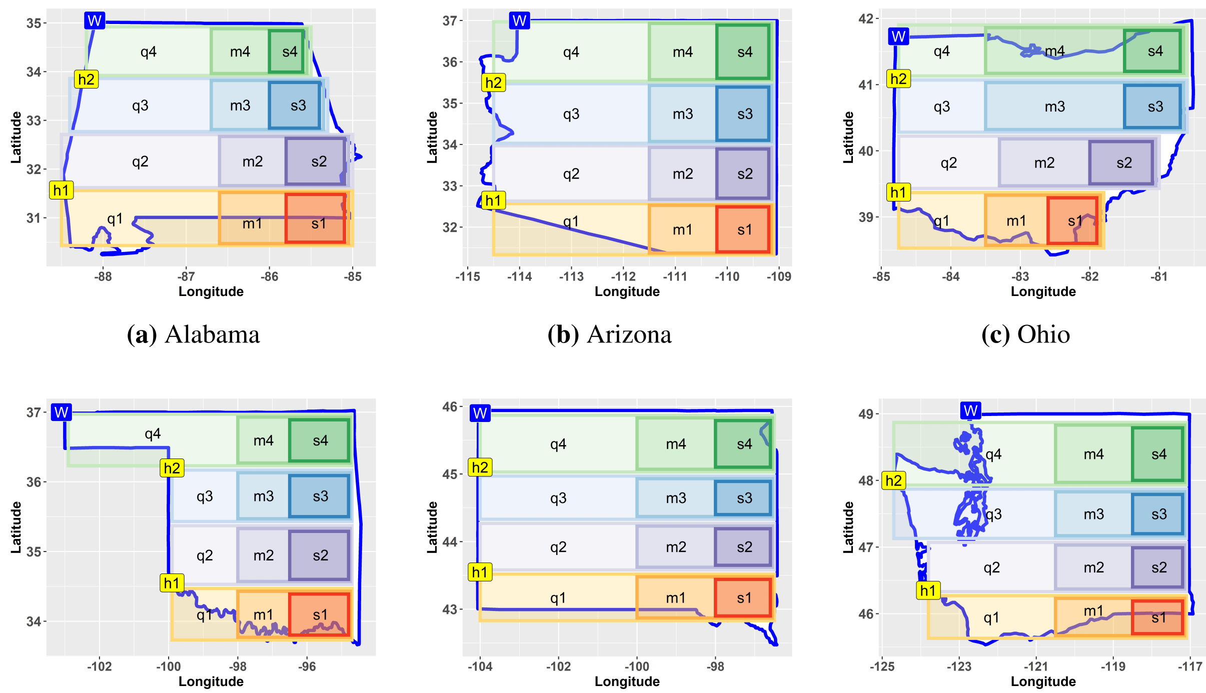

(a) Alabama **(b)** Arizona **(c)** Ohio

(d) Oklahoma **(e)** South Dakota **(f)** Washington

Figure 2.2: Regions used for analyzing the effect of pooling

Step 1 *Select a harvesting state.* For this case study we arbitrarily picked six states spread across the continental US: Washington, South Dakota, Ohio, Arizona, Oklahoma and Alabama. These were selected as large representatives of different US geographical regions. We chose not to perform the analysis for all states, in order to allow for presenting results for each separately.

Step 2 *Split the harvesting state into harvesting regions of varied size.* Specifically, we use the following procedure, illustrated in Figure 2.2. First, the state in itself represents a harvesting area, labeled *whole*. It is then split vertically in half, creating two *half* areas. Each half area is then split vertically in two resulting in two *quarter* areas (four in total). Each quarter is then split in half horizontally creating four *medium* areas, which are finally split in half for four *small* areas. This allows us to test the connection between the harvesting area size and the effect of pooling across different geographical regions.

Step 3 *Select generation sites.* For the selected harvesting area, we identify wind generating locations. Figure 2.3 shows selected wind sites in each state. The generation sites are sampled from the ones available in the NREL dataset. Note that we chose not to use all of the locations for computational tractability. Instead we sample from the list of given sites so that the resulting generation sites are distributed across the whole state as uniformly as possible. As a way to illustrate

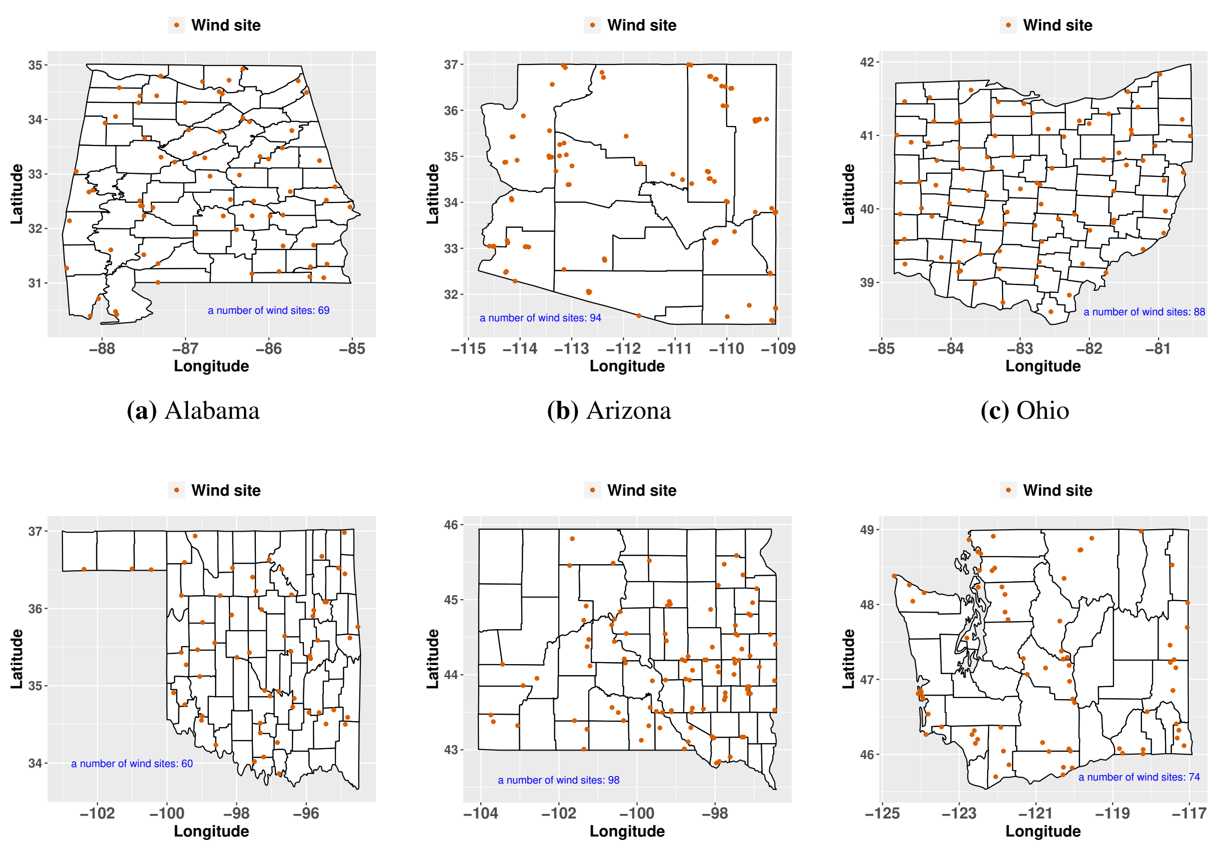

(a) Alabama **(b)** Arizona **(c)** Ohio

(d) Oklahoma **(e)** South Dakota **(f)** Washington

Figure 2.3: Wind sites used for in the case study.

the properties of the generation profiles in the selected sites, Figure 2.4 depicts the average and standard deviation of hourly generation for each site in each state. We can observe that most exhibit relatively large variance, and hence can be characterized as highly intermittent. The average (over each state locations) relative day ahead forecasting error varies from 32% (Oklahoma) to 52% (Arizona).

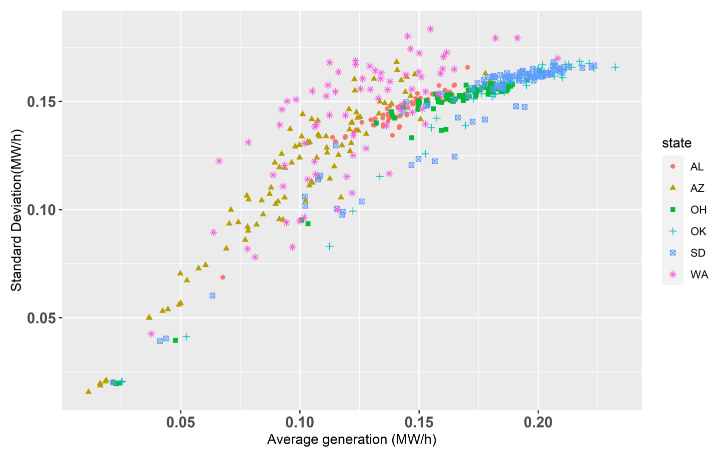

Figure 2.4: Average and standard deviation of hourly generation of all selected sites.

Step 4 *Find a set of optimal generation portfolios for the selected harvesting area.* The optimal portfolios are identified by solving the optimization problem described above. Parameters, α and A_0 are set as $\alpha = 0.1, 0.5, 0.9$, and $A_0 = \gamma \max_{i \in 1\ldots n} \bar{A}_i$, with $\gamma = 0.1, 0.2, 0.3, 0.4, 0.5, 0.7, 0.8, 0.9,$ $0.95, 0.99$. Naturally, this way of selecting A_0 allows for varying the optimal portfolio average generation from the best possible ($\max_{i \in 1\ldots n} \bar{A}_i$) to the worst. For example, $\gamma = 0.9$ will result in a portfolio that on average produces at least 90% as much as the location with the highest average generation. All underlying linear programming optimization problems are solved with IBM ILOG CPLEX Version 12.7.1 [57], on a desktop computer with Intel Core i5 processor and 8GB of RAM. Each run required approximately 180 seconds per portfolio.

Step 5 *Evaluate generation profile for each optimal portfolio in each harvesting region.* Each optimal portfolio generation is then evaluated over the testing time period. The relative forecasting error δ is defined as the ratio between portfolio forecasting error (ε_j) and its generation, averaged over the testing period.

2.4 Results of the case study and discussion

The obtained optimal portfolios are compared against two benchmarks: *individual generation sites*, and *equal weight portfolio*. Each individual location can be viewed as a (non-pooled) portfolio with $x_{i_0} = 1, x_i = 0, \forall i \neq i_0$ for the corresponding i_0. In this context the difference between the generation profiles from the single-location portfolios and the optimal CVaR portfolios provides evidence for the effect of pooling. Equal weight portfolio is defined as $x_i = \frac{1}{n}$, where n is the number of wind generation locations in the area. This approach can be viewed as representing unplanned development, where each available location is considered independently, without overarching design. Comparing the profile of equal weight approach to the optimal CVaR portfolios allows for evaluating how much of the pooling effect can be increased by intelligent planning, as opposed to a naturally occurring outcome.

2.4.1 Effect of pooling

Figure 2.5 summarises the effects observed on the state level. Specifically, it depicts the performance of the three types of portfolios (optimal CVaR in blue, equal-weight in red and no-pooling in green) in terms of the average generation and relative forecasting error δ for each of the studied states. Note that for the pooled cases (CVaR and equal-weight) the values observed in each testing year (2009-2012) separately are plotted. The metrics for the no-pooling cases (individual generation locations) are evaluated over the whole testing period (4 years) in order to avoid having to

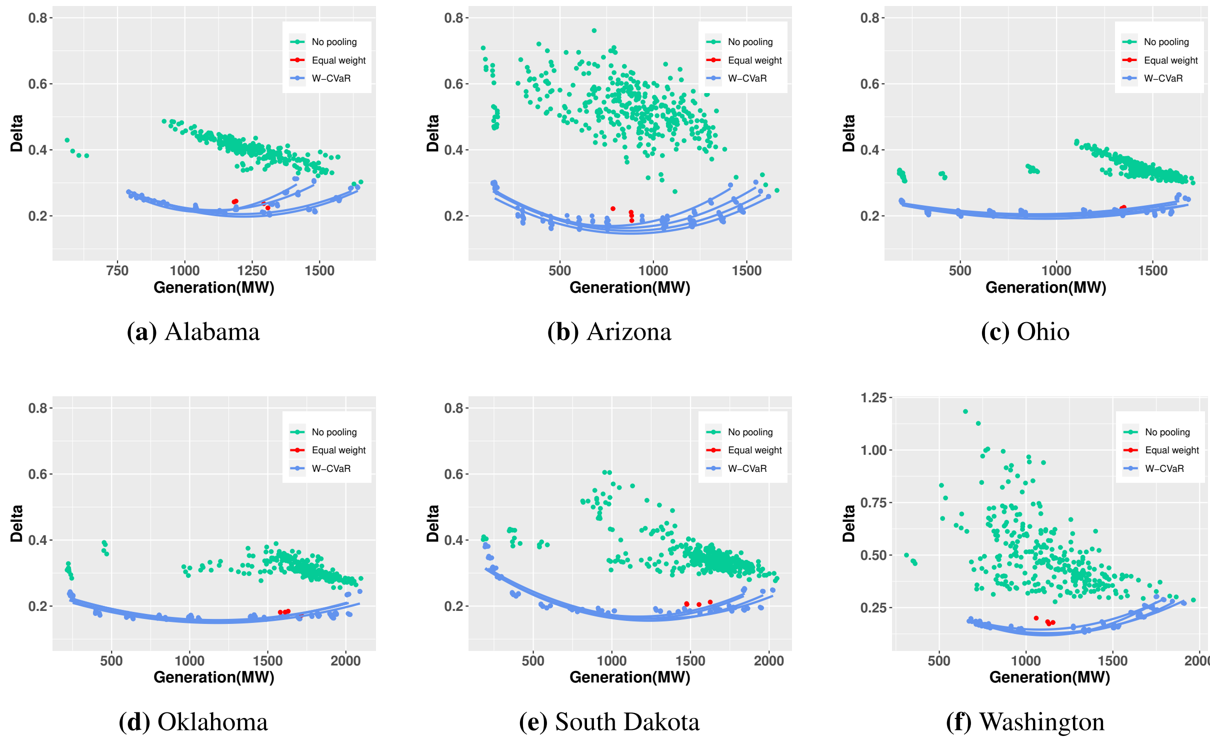

(a) Alabama **(b)** Arizona **(c)** Ohio

(d) Oklahoma **(e)** South Dakota **(f)** Washington

Figure 2.5: Results comparing the optimal portfolio performance for the six states considered.

plot too many observations on the graphs. Observations corresponding to the optimal CVaR portfolios are also supplemented with approximating lines (one for each testing year), obtained by fitting polynomial regression. These can be viewed as depicting the trade-off between forecasting error and average generation. Naturally, the value of parameter γ explicitly determines the position of a CVaR portfolio on this curve. Table A.2 in the Appendix provides the same information, focusing on average, minimum and maximum δ in each state across the portfolio types. In the table the minimum, maximum and average errors for the high-generation CVaR optimized portfolios ($\gamma = 90\%$) are reported separately.

First, observe that in all states and all testing years the lowest error is achieved by one of the CVaR-optimized portfolios. While this is not surprising in itself (the portfolios are designed to have the smallest possible error albeit over the training set), it is worth emphasizing that in all states tested the improvement compared to non-pooled cases is substantial, with optimization being able to reduce the minimum forecasting error up to two times (or more). Further, while, naturally, pooling reduces the maximum possible expected generation (due to mixing high-producing and low-producing locations together), most of the improvement in forecasting error can be achieved by sacrificing only 10% of average generation (compare portfolios corresponding to $\gamma = 0.9$ with the best performing individual locations in Table A.2). Depending on the practical case in question 10% may or may not be an acceptable loss. In contrast, if γ is 0.99, δ are almost the same as that of the facility with the maximum output since pooling is severely limited in this case. Consequently, it must be emphasized that reduction in average generation compared to the best-performing location is an unavoidable consequence of pooling.

Considering the equal-weight portfolio it can be observed that even this naive approach is capable of substantially reducing the forecasting error by itself. At the same time, it is worth emphasizing that optimized portfolios may retain two important advantages. First, observe that in some cases, e.g., Ohio and South Dakota, equal weight approach remains competitive in terms of average generation. On the other hand, in the case of Arizona and Washington these result in very low average generation values, which can be unacceptable. Most importantly, the optimization-based approach enables the decision maker to balance forecasting error and average generation, which is impossible in the case of unplanned development. Secondly, it must be noted that CVaR optimization naturally restricts the number of sites that need to be invested in order to reduce the error. Table 2.1 reports the average proportion of candidate locations that are included in the optimal portfolios. While for smaller regions with limited diversification options almost all of the locations are used, in all state-wide examples not more than 23% are needed. On the other hand, an equal weights portfolio requires investment in all candidate locations. The number of candidate locations is naturally related to capital investment costs, and hence, this could be viewed as a potentially significant benefit of portfolio optimization approach.

State		Region 1	Region 2	Region 3	Region4	State		Region 1	Region 2	Region 3	Region4
Alabama	small	96.0(5)	93.3(6)	90.0(4)	100.0(2)	Arizona	small	62.9(7)	50.0(6)	100.0(1)	60.6(8)
	medium	81.7(9)	75.0(12)	76.7(9)	81.9(8)		medium	63.1(8)	47.8(9)	45.6(9)	25.8(18)
	quarter	62.3(15)	51.7(21)	55.9(17)	61.6(16)		quarter	45.9(16)	29.8(22)	28.9(31)	24.8(25)
	half	41.7(36)		39.5(33)			half	28.0(38)		18.9(56)	
	whole	21.5(69)					whole	16.5(94)			
Ohio	small	76.0(5)	78.6(7)	90.0(6)	86.7(6)	Oklahoma	small	-(0)	85.8(6)	67.8(9)	86.3(4)
	medium	57.8(9)	71.4(11)	61.0(15)	56.7(12)		medium	73.0(5)	53.3(12)	48.8(13)	77.2(9)
	quarter	47.7(15)	49.2(24)	46.1(28)	46.4(21)		quarter	67.5(6)	52.8(18)	43.2(19)	50.6(17)
	half	28.6(39)		26.1(49)			half	35.8(24)		31.8(36)	
	whole	19.5(88)					whole	23.0(60)			
South Dakota	small	70.0(8)	38.8(17)	71.4(7)	81.0(5)	Washington	small	64.3(7)	67.5(4)	95.0(4)	93.3(3)
	medium	22.7(24)	25.7(29)	40.7(14)	69.2(6)		medium	49.3(14)	50.6(8)	72.8(9)	68.9(9)
	quarter	25.9(33)	26.6(35)	34.0(21)	70.0(9)		quarter	42.7(22)	31.1(18)	69.6(13)	43.1(21)
	half	17.5(68)		33.2(30)			half	27.8(40)		39.0(34)	
	whole	15.1(98)					whole	21.2(74)			

Table 2.1: The average proportion of facilities pooled among the available locations in optimal portfolios. The values are reported in percent and the total number of potential locations is given in parenthesis.

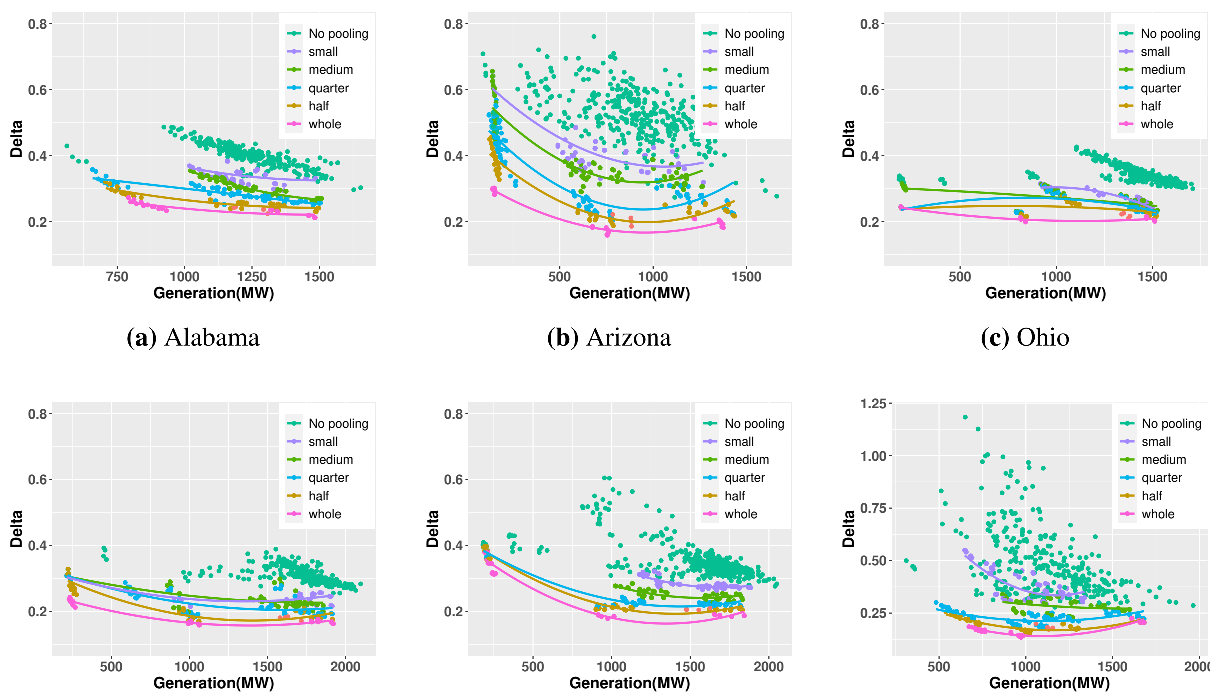

(a) Alabama **(b)** Arizona **(c)** Ohio

(d) Oklahoma **(e)** South Dakota **(f)** Washington

Figure 2.6: Effect of harvesting region size on the achieved forecasting error. All pooled and non-pooled portfolios are evaluated in terms of average generation and relative forecasting error.

2.4.2 Effect of harvesting area size on benefits due to pooling

As discussed above, smaller regions should generally correspond to more correlated outputs, and hence tend to have less potential for effective pooling. It is important to note that each area has different intrinsic potential for wind energy generation, and our focus is on identifying states that are particularly promising in terms of reducing the forecasting error and not necessarily the actual generation. First, consider Figure 2.6 and the corresponding Table A.3. Similarly to Figure 2.5 above here the observed forecasting error (δ) and average generation for the optimized and no-pooling portfolios are depicted. To avoid overcrowding the graphs, here we only depict the portfolios designed to achieve 90%, 50% and 10% of the maximum average generation and the corresponding regression lines. The observations are grouped (and colored) according to the size of the harvesting regions.

Most importantly, in all tested states it can be observed that a larger harvesting region directly leads to lower forecasting error. This is evidenced by monotone decreasing values for the minimum, maximum and average delta for almost all states and testing years as we move from small areas, to medium, to quarter, to half and to whole states in Table A.3 and in the corresponding regression lines in Figure 2.6. In some states (particularly, Arizona and Washington), the difference between the pooling effect on different scales is especially pronounced. For example, by expanding the harvesting region from a small (county-size) area to the whole state, the minimum forecasting error in Washington (in 2009) reduces from 40% to just 19% (the effect is similar in the other testing years). On the other hand, in some states, this effect is less important (see, for example, Ohio). This then suggests that different geographical areas respond differently to the size of the pooling region.

The observations above are further supported by Figure 2.7 and the corresponding Table 2.2. Here the minimum forecasting error achieved by the optimized portfolios on each of the harvesting regions is plotted against the size of the region (measured as the maximum distance between two generation locations) along with the fitted linear regression lines. The regression coefficient and its p-value as well correlation coefficient are also reported. All slopes observed are negative with the corresponding $p << 0.05$. The regression slope can be naturally interpreted as the expected reduction in average forecasting error after an expansion of the diameter of the harvesting region by 1km. In other words, according to our experiments, 100km expansion of the diameter of the harvesting region reduces the relative forecasting error by 4% in Washington; by 2% in Alabama, Arizona, South Dakota and Oklahoma; and by 1% in Ohio.

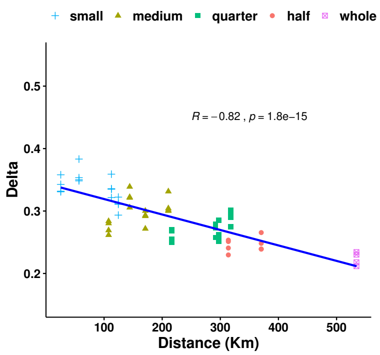

(a) Alabama

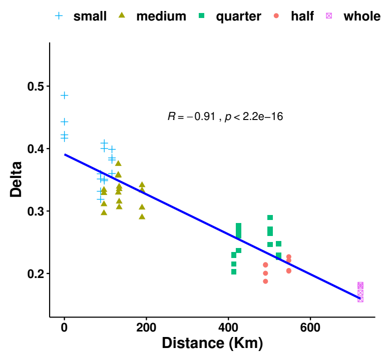

(b) Arizona

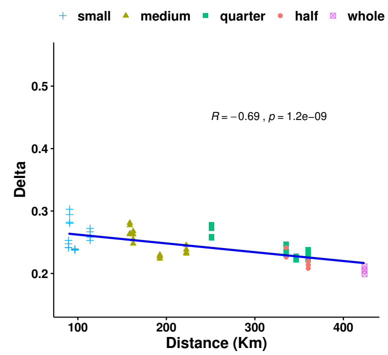

(c) Ohio

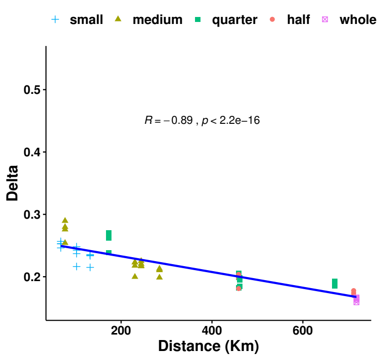

(d) Oklahoma

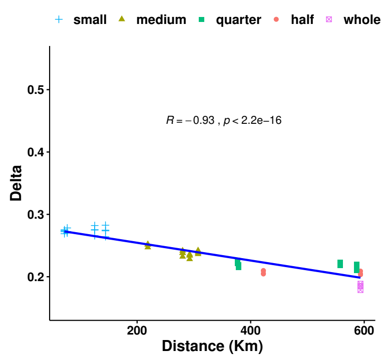

(e) South Dakota

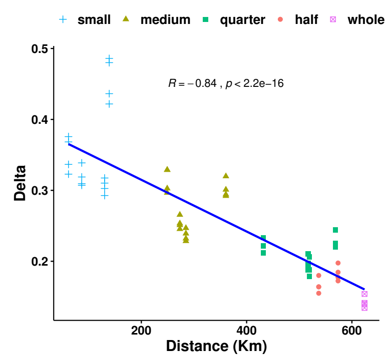

(f) Washington

Figure 2.7: The minimum achieved forecasting error in optimal portfolios plotted against the harvesting area diameter (measured as maximum distance between generation sites) with fitted linear regression trend.

State	Trend line equation	State	Trend line equation
Alabama	*Error* = 34.13 - 0.02 *Diameter*	Oklahoma	*Error* = 26.69 - 0.01 *Diameter*
Arizona	*Error* = 42.00 - 0.02 *Diameter*	South Dakota	*Error* = 28.82 - 0.01 *Diameter*
Ohio	*Error* = 28.13 - 0.01 *Diameter*	Washington	*Error* = 40.27 - 0.04 *Diameter*

Table 2.2: Summary of the linear regression trend lines on Figure 2.7

2.4.3 Application to battery sizing problem

To better illustrate the potential for practical significance of forecasting error reduction we also include a small-scale "proof-of-concept" experiment, aimed at outlining the effect of forecasting error reduction on a simple generation planning problem. It should be emphasized that this discussion is presented as an illustration and a more comprehensive evaluation of the effect of variability reduction on electricity generation is beyond the scope of the current effort and should be a topic of a future study.

We derive the optimal generation portfolio from the proposed mean-CVaR model based on historical data similarly to the results discussed above. Here we randomly select 10 on-shore locations in the State of California. The optimal portfolio or one of the 10 individual locations' portfolio generation profiles are then fed into a typical cost minimization problem for a microgrid. The microgrid is assumed to be connected to the external grid and the corresponding optimization problem is concerned with sizing a battery storage with the goal of minimizing operation cost, while satisfying demand with either renewable generation or from the external grid. We use a simple generation planing problem, presented in detail in A.1, with realistic but simplified assumptions on model parameters. The model and parameter values are selected closely following the experiments presented in [58, 59]. Specifically, the microgrid is assumed to consist of a collection of residential houses, each with typical demand pattern as given in [60]. The number of households is selected to match the total average demand with the average renewable generation (i.e., on average the total annual demand is equal to the total annual generation). Batteries used are assumed to be household batteries with parameters as described in [61]. To simplify the model we further assume constant sale and purchase price on the external grid, estimated following the average values reported in [60]. Note that this implies that here the microgrid cannot profit from buying external energy during low cost periods to store and then sell it during high cost periods, i.e., batteries can only be

Portfolio	Total Cost ($)	Battery modules	Wind energy (Kw/year) (including Battery energy)	Grid energy (Kw/year)
pooled	135,286	1,518	29,200,673	7,376,417
location 1 only	364,580	638	16,293,486	20,021,275
location 2 only	320,953	3	18,127,702	18,216,809
location 3 only	368,542	3	15,626,303	20,668,178
location 4 only	258,494	1,806	21,757,547	14,671,676
location 5 only	263,129	1,861	21,313,381	15,110,254
location 6 only	457,719	337	11,488,490	24,724,990
location 7 only	299,016	1,943	20,610,147	15,797,622
location 8 only	391,247	3	14,656,091	21,618,985
location 9 only	169,891	358	25,168,309	11,320,370
location 10 only	291,154	3	19,367,532	17,001,766

Table 2.3: Result of battery sizing experiment for pooled and 10 non-pooled cases.

profitably used to store renewable energy. The renewable generation data used is from the same source as the main experiment. For completeness, relevant parameter values are given in A.1.

Figure 2.8 and Table 2.3 summarize the results obtained. Figure 2.8 depicts a week (during the testing period) of the generation from the 10 renewable locations, the generation from the optimal portfolio ($\alpha = 0.9$ and A_0 selected as the average demand level) and the total demand. Table 2.3 reports the optimal size of the battery selected (measured in the number of standard modules), total cost and the split between renewable and grid energy used to satisfy the demand for each of the individual locations and the optimal portfolio. Most importantly, observe that indeed the optimized portfolio uses the least amount of grid energy and achieves the lowest total cost. Somewhat counter-intuitively, it also requires a significant investment into battery capacity, but this observation can be explained by noting that due to the lower overall variability it is able to use the available battery resources more efficiently, and hence the additional investment is justified by the lower cost of grid exchange. It should be emphasized that this experiment does not constitute a comprehensive evidence for the benefits due to reduced variability, and instead we only present it here for illustration purposes.

2.5 Concluding discussion

The study introduces a new modeling approach aimed at evaluating the effect of pooling geographically diverse wind generation locations in order to reduce forecasting error. The model,

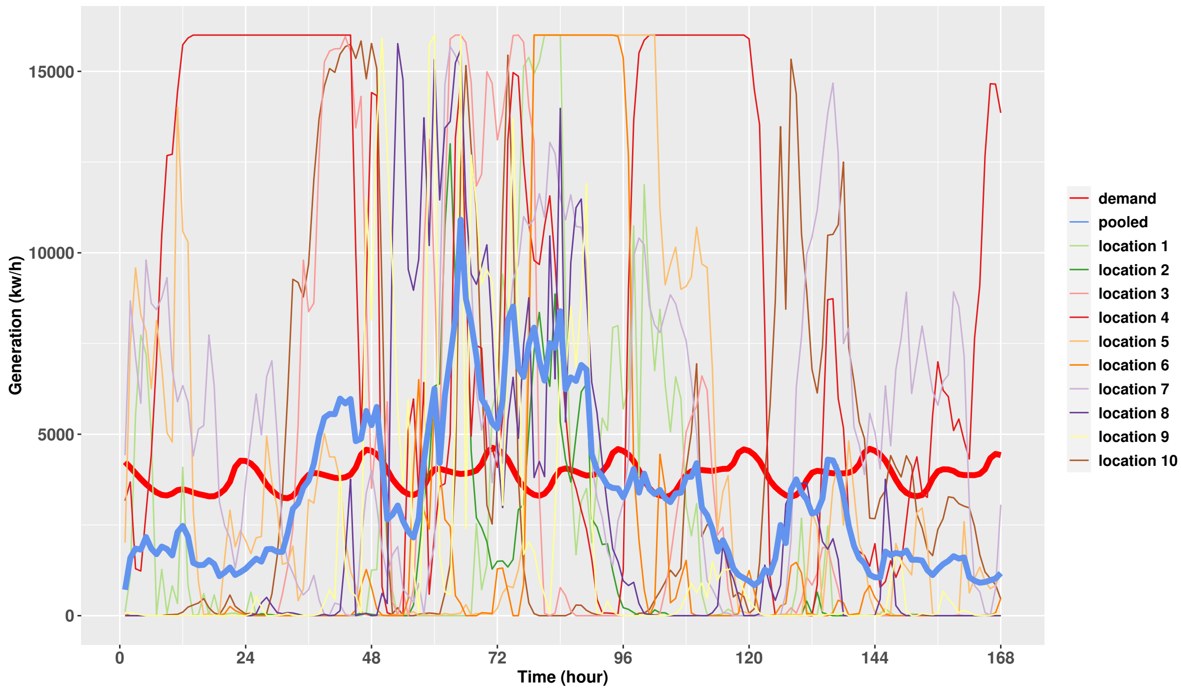

Figure 2.8: Demand and generation profiles for 1 week of testing period for the optimal portfolio and individual locations.

constructed as a mean-CVaR optimization problem, provides a family of optimal generation portfolios for a pre-determined harvesting region, which are designed to take advantage of the correlation structure in the generation and forecasting profiles in order to reduce the overall error, while maintaining satisfactory expected generation. It is then used to evaluate the potential effect of such a technique in a case study based on real data from US states.

Most importantly, the results have shown that pooling can substantially reduce the forecasting error of wind energy generation, up to 50% when pooled across a whole state compared to no pooling. While the scale of this reduction is different in different states considered, in all cases it is substantial. Consequently, we conclude that while for majority of individual wind generation locations generation may be hard to predict, the forecasting error can always be significantly reduced by pooling from geographically distant sources. The approach allows for quantifying the effect of geographical size of the harvesting region on error reduction. On average, 100km increase in area diameter results in 1%–4% of reduction in average relative forecasting error, depending on the region studied.

It is also observed that a significant portion on this improvement can be realized even without advanced optimization tools. Particularly, equal weight portfolios, aimed at simulating unplanned development, in most cases exhibit significant reduction in forecasting error. At the same time, the proposed optimization approach outlines the underlying trade-off between average generation and forecasting error. Intuitively, the highest average generation can be achieved if investment is concentrated in a handful of most productive locations, while in order to reduce the forecasting error the decision maker should spread the investment across a diverse set of generation profiles. It is demonstrated that any time many geographically distant locations are pooled together, the forecasting error is reduced (the equal weight portfolios in the case study), yet this approach may result in significant loss in average generation potential. The proposed model illustrates that with a carefully designed optimization problem it is possible to achieve the same or better forecasting error, while managing average generation at the same time.

The outcomes of the case study serve to highlight the important role that pooling plays in forecasting error magnitude in wind generation. The primary driving factor of this effect is the size of the geographical area used for harvesting. While significant error reduction happens naturally as geographically diverse locations are pooled together, it may be further beneficial to incorporate a more advanced portfolio optimization approach, such as the one proposed here, since it can allow for balancing the average generation and forecast, in addition to achieving diversification with a fewer number of pooled locations by proactively taking advantage of the underlying correlation structure. These considerations are important in capital planning and generation expansion problems. Particularly, it can be adapted for design problems related to virtual power plants (VPPs), since these can explicitly consider energy portfolios and rebalance them relatively often. Additionally, our proposed approach can be closely relevant to battery sizing problems since the lower overall forecast error can directly translate to either lower capacity requirement or its more efficient use, and hence better return on the investment, and ultimately, wider use of renewables. Further, the observations made can be relevant for research into innovative ways to integrate renewable energy generation as a significant part of the overall portfolio, such as wind farm coalitions, cooperation between microgrids, or smart grid design.

A number of the study limitations and directions for future research must be emphasized. First, observe that transmission considerations pose a significant factor directly relevant to practicality of pooling. Naturally, pooling from a larger harvesting region can require transmission over longer distances, leading to transmission losses, which, in turn, reduces the overall system efficiency. Further, and potentially more importantly, the transmission network structure can significantly reduce feasibility of pooling from the technical implementation perspective. For example, generation and demand balancing may be administered per each transmission node separately through directly connected parties severely restricting pooling options. Transmission factors are not included into our model, and consequently, the presented results can be viewed as measuring the potential benefits due to pooling, which may not be fully realizable in a practical system. This modeling choice is made to allow for computational tractability as well more streamlined interpretation of the results without making additional assumptions on the transmission network. Note that the effect of these factors significantly depends on the particular system design. For example, a VPP may be less sensitive to them due to its virtual nature. A careful analysis of the effect of pooling, given a particular transmission system design and the interests of all demand balancing parties (retailers, aggregators, generators, etc) could be a topic of a future study. An example of a research effort in this direction, which considers a simplified transmission network is given in [62], albeit concentrating on reduction in intermittency.

A careful economic cost-benefit analysis of explicitly considering forecasting error reduction techniques in capital planning or VPP investment problems is beyond the scope of what can be done with the proposed model directly. At the same time, the proposed approach can be incorporated into such an analysis, which would take into account the design of a particular transmission network, energy market conditions and polices, storage availability, etc.

Furthermore, a similar set of experiments could be performed with solar generation or any other variable energy source. Given the diversity in the underlying technology, and hence relative independence of both average generation and forecasting error, including solar into the mix can only increase the benefit of pooling. The extent of this improvement can be evaluated in a future study.

Finally, an interesting question not considered here is the interaction of the effects that pooling diverse energy sources has on intermittency and predictability. As discussed in the introduction, both are important factors limiting applicability of renewables. At the same time, both are affected by the same mechanism of risk reduction through diversification when pooled from geographically diverse areas. Consequently, a study into the extent to which both can be improved at the same time through careful planning is needed.

Chapter 3

Optimize the energy storage capacity through portfolio optimization in micro grid system

3.1 Introduction

Energy storage is the most readily apparent tool for mitigating wind power intermittency and load mismatches when renewable energy is integrated in a microgrid. Specifically, the Energy Storage System (ESS) plays important role in mitigating wind power intermittencies through charging and discharging the energy to satisfy the demand in a microgrid to match the time periods when energy is needed with time periods when it is produced. Further, ESS can provide reliability (consistently delivering high-quality power), resilience (maintaining critical function and quick recovery), and flexibility for remote communities and targeted microgrid solutions ([63]). At the same time, due to significant cost of the hardware involved, the sizing of ESS to enable these benefits remains a significant problem to be solved when designing a microgrid.

It is natural to expect that reducing both intermittency and unpredictability of renewable generation through pooling may directly lead to a reduction in the battery capacity requirement. In this chapter, we propose a heuristic approach to reduce the energy storage capacity through portfolio optimization of wind energy composition used to power the system. Specifically, a proposed heuristic approach is a series of procedures that derive portfolios that minimize forecasting errors through risk-averse models (following the approach proposed in the previous chapter) and then optimize battery capacity and total operating costs given the output of this optimized portfolio.

We then investigate the impact on battery size and operation planning costs, and different types of wind energy portfolios (onshore, offshore) and geographical regions (California and Wyoming in this case) on the benefits due to pooling in a numerical case study.

A number of algorithms and methodologies have been proposed to optimize ESS capacity in microgrids given either deterministic or stochastic model for renewable generation. For example, [58] used a dynamic programming algorithm to maximize the expected profit over the scheduling period by determining the optimal energy exchange with the market for a specified scheduling period with a properly sized energy storage. In [64], the tabu search (TS) methodology is used to maximize the benefits of the power supply-side. A thermal unit commitment program considered the demand response system to satisfy the transmission constraints and included the goal of reducing energy storage system (BESS) capacity. In [65], the authors used a mixed-integer linear programming method to minimize the total cost by optimally sizing an ESS to be integrated with a grid-connected microgrid. In [66], a self-adaptive hybrid optimization algorithm is used to minimize the operating cost of EV charging stations integrated with PV and ESS. Quadratic programming (QP) was used in [67] in order to improve integration of renewables into the electricity grid and an optimal design of a storage system is performed. Specifically, two ways of increasing the integration of wind and solar energy into the electricity grid through energy storage were analyzed. The first service to the electricity grid is related to a smoothed and hourly scheduled daily production while the second one concerns a constant and guaranteed minimal production. The authored of [68] used model predictive control (MPC) methodology which considers the future wind power predictions and state of charge (SOC) of BESS to implicitly to minimize the operation cost. In [69], particle swarm optimization is used to maximize the system energy production and meet the load demand with minimum cost and highest reliability. The authors employed demand profiles using load shifting-based load priority which is either High (fixed scheduling requirements) or Low (flexible scheduling requirements). In [70], the authors used Integer Nelder-Mead algorithm and simplex method to find a local minimum to determine a cost-efficient solution to sizing the PV system with maximizing the operation of higher priority appliances. However, most of the existing research does not focus on renewable energy supply part to reduce the storage capacity but rather recognizes it as uncertain but fixed.

In contrast, this chapter assumes that the renewable energy composition sometimes can be considered as a decision variable, i.e., it is possible to adjust the renewables generation profile by mixing together the generation from disparate sources. Consequently, we investigate to what extent optimization of this portfolio can be helpful in reducing investment and/or operational costs. Note that the assumption described may be particularly suitable in two cases: a VPP or a microgrid. As was discussed in Chapter 1, VPPs are often able to frequently rebalance their generation portfolios, and hence can naturally take advantage of any pooling effect as studied here. Similarly, a microgrid may be able to contract with multiple disparate generation sources to create its energy portfolio. While we will concentrate on a VPP as a use case in the next chapter, in this chapter we will assume a microgrid case.

From the methodological perspective the proposed model is a two-stage optimization problem, where on the first stage the generation portfolio is selected, and then on the second stage an ESS sizing problem similar to the ones discussed above is solved. Naturally, this can be a challenging problem computationally, and consequently, first we investigate a heuristic approach to solving it, whereby the stages are separated and solved one after the other.

Consequently, the goal of this effort is to consider the following two research questions:

- What is the impact of an optimized pooled portfolio for smart grid system reliability;
- How much is it possible to reduce the energy storage system size through the optimal portfolio;

To this end, we design a simulation study, based on risk-averse portfolio optimization with Conditional-Value-at-Risk(CVaR) and mixed-integer linear programming model. We obtain optimal pooling results using mean-CVaR model and then derive optimal operation planning (battery size, total cost, etc.) in MILP utilizing pooling results as input.

The contributions of the research effort are as follows:

- we propose a general two-stage model for optimized energy portfolio selection and battery sizing;
- we then consider a heuristic approach to solving the two stage model;
- we finally employ the model and solution approach to conducting numerical experiments demonstrating the extent to which optimized pooling can reduce the costs associated with ESS investment.

The remainder of the chapter is organized as follows. Section 3.2 describes the proposed microgrid system. Section 3.3 presents the proposed risk-averse optimization and MILP model with the mathematical formulation. Section 3.4 explains the system data for case study. Section 3.5 discusses the case study and the results. Finally, Section 3.6 concludes the discussion and outlines some ideas for future research.

3.2 Microgrid system description

Figure 3.1 describes the scheme of the microgrid and proposed management system for reducing the battery capacity. We assume that a microgrid is composed of a portfolio of wind power plants (onshore and/or offshore) as integrated renewable energy sources, storage, external grid, market, and energy consumed by residential buildings. In other words, the microgrid is assumed to be connected to the external grid and the corresponding optimization problem is concerned with sizing battery storage with the goal of minimizing operational cost while satisfying demand with either renewable generation or external grid.

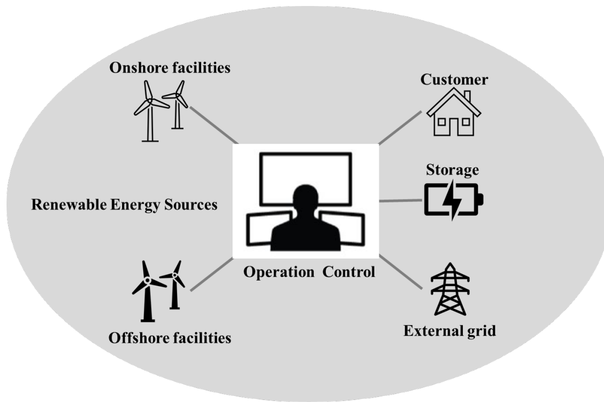

Figure 3.1: Scheme of the assumed microgrid.

3.2.1 Wind power plant

It is assumed that wind facilities generate energy as renewable energy sources. We include both onshore and offshore options to be able to compare their relative effect. We further consider onshore facilities, producing according to generation patterns found in two separate geographic areas (California and Wyoming), to investigate the effect of geographical diversity. We do not include solar energy since no forecasted data has been available to the authors with sufficient time and spatial resolution.

3.2.2 Energy storage system

Renewable technologies require energy storage to facilitate intermittency and ensure safe delivery. We assumed residential lithium-ion battery as storage to complement intermittency since it is the cheapest and most widely used [71]. The battery supplies stored energy to meet the demanded load when the available wind energy is insufficient.

3.2.3 Customer

We assumed that customers are represented by a group of households, consuming wind energy hourly from either the wind farm, storage or external grid to meet the demanded load.

3.2.4 External grid

It is assumed that the microgrid is connected to the external grid for delivering electricity to consumers or selling the excess energy to the market. For simplicity, we assume that there is no energy lost due to transfers.

Indices		$capa^{dchr}$	maximum discharging power (%)
i	house (i = 1...I)	IOC	initial SOC in the battery (%)
t	time (t = 1...T)	SOC^{min}	minimum state of charge (%)
		SOC^{max}	maximum state of charge (%)
Parameters			
AEC^{bat}	annual equivalent cost of battery (cent)	Variables	
$P_{i,t}^{grid}$	grid cost in house i during period t (cent)	x_{bat}	integer variable to indicate the Number of the battery
S^{price}	wholesale wind energy price (cent)	$E_{i,t}^{grid}$	used grid energy in house i during period t (kwh)
E_t^{wind}	wind energy output during period t (kwh)	E_t^{sell}	selling wind energy during period t (kwh)
$D_{i,t}^{house}$	energy consumption in house i during period t (kwh)	$E_{i,t}^{rewH}$	used wind energy in house i during period t (kwh)
INV^{rate}	Invereter efficiency (%)	E_t^{chr}	charge energy in the batter during period t (kwh)
E_t^{limit}	limited selling energy during period t (kwh)	$E_{i,t}^{dchr}$	Discharge energy in the batter to house i during period t (kwh)
$dchr^{rate}$	self-discharging efficiency (%)	E_t^{bat}	available energy in the battery during period t (kwh)
chr^{rate}	charging efficiency (%)	y_t^{chr}	binary variable variable to indicate charging state during t
C^{bat}	capacity of single battery module (kwh)	y_t^{dchr}	binary variable variable to indicate discharging state during t
$capa^{chr}$	maximum charging power (%)		

Table 3.1: Nomenclature for the proposed operational planning model

3.3 Research methodology

The study proposes a heuristic approach to reduce battery capacity and system total cost through selection of both renewable energy portfolio and operational controls. Figure 3.2 and Figure 3.3 describe the approach and flowchart of the heuristic methodology based on similar mean-CVaR model as in the previous chapter. Specifically, first we find the optimal renewable energy portfolios from risk-averse optimization model based on the expected demand load. Next, we evaluate the system cost through operational planning problem using an optimal generation profile created from mean-CVaR model for a year (8764 hours). Detailed formulations and methods will be described in the following section.

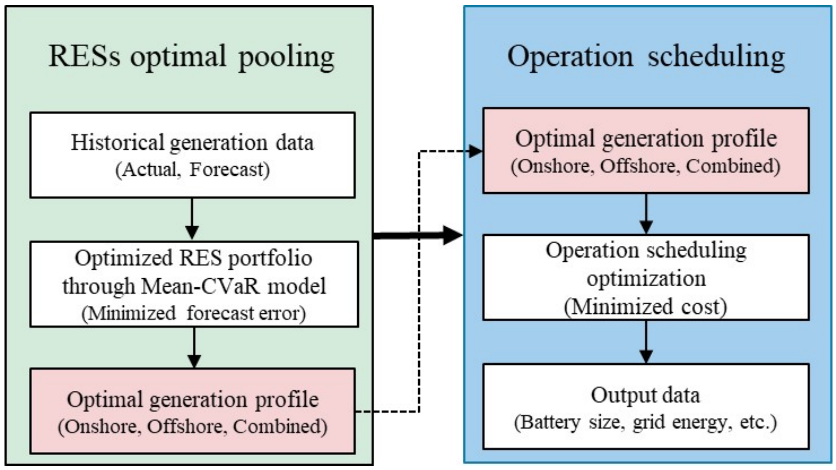

Figure 3.2: Proposed optimization framework

3.3.1 Risk-averse optimization model

The portfolio construction methodology is based on risk-averse stochastic optimization, mean-Conditional Value-at-Risk (mean-CVaR), and the training-test framework as discuss in Section 2.3.4 in Chapter 2, restated here for the sake of completeness as follows.

$$\min_{\eta\in\mathbb{R},\mathbf{w}\in\mathbb{R}^m,\mathbf{x}\in\mathbb{R}^n} \quad \eta + \frac{1}{(1-\alpha)m}\sum_{j}^{m} w_j \tag{3.1}$$

$$\sum_{i}^{n} x_i = 1 \tag{3.2}$$

$$\sum_{i}^{n} \bar{A}_i x_i \geq A_0 \tag{3.3}$$

$$w_j \geq -\Big|\sum_{i=1}^{n}(A_{ij} - F_{ij})x_i\Big| - \eta \tag{3.4}$$

$$\mathbf{x}, \mathbf{w} \geq 0 \tag{3.5}$$

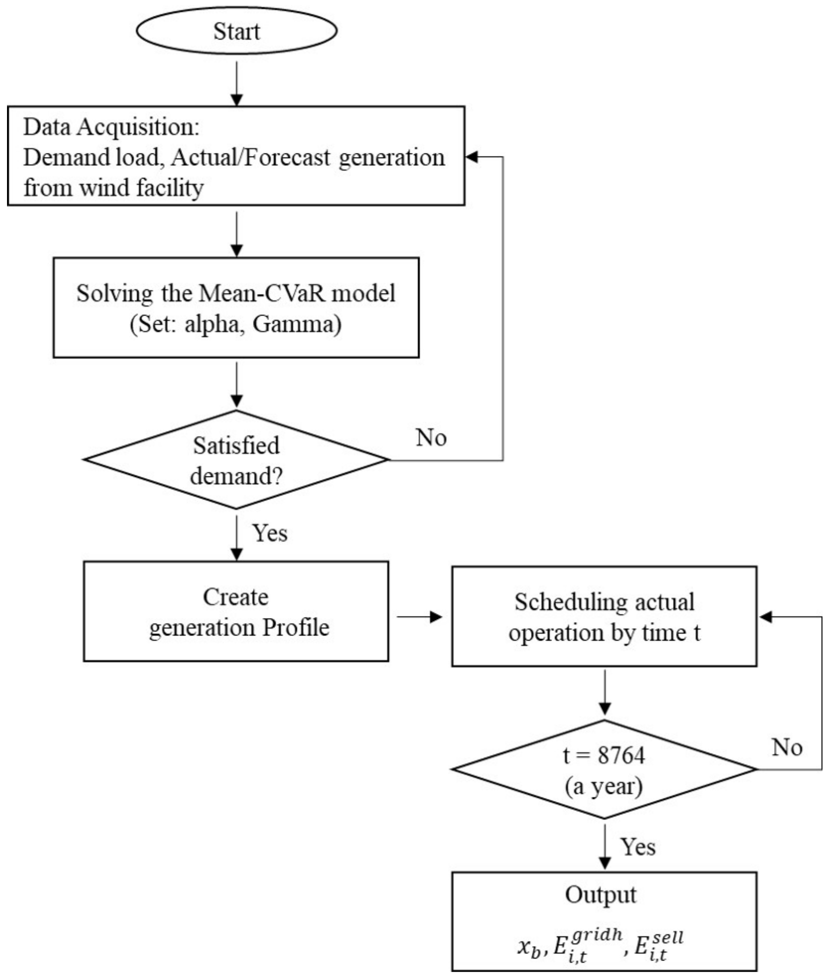

Figure 3.3: Flowchart of the proposed heuristic method for solving the bi-level problem.

Recall that A_0 denotes the target average generation. Naturally this parameter is related to the expected hourly demand and so is set accordingly in our case study.

3.3.2 Operation planning model for energy management

The operational planning model describes the interaction between storage (battery), customer (demand) and external grid (market). The decision making problem here is to select the size of the battery that minimizes the total annual cost, which consists of the battery investment and operational costs. The operational costs consist of the energy bought (and sold) on the market under the realized renewable generation scenarios.

Objective function The goal of the optimization model is to minimize the total cost (C), which consists of two components: annualized battery investment cost and the balance between purchasing and selling the energy to the market. The objective then can be expressed as follows.

$$\min C = \quad AEC^{bat} \times x_{bat} + \sum_{i=1}^{I} \sum_{t=1}^{T} \left(E_{i,t}^{grid} \times P_{i,t}^{grid} - \sum_{t=1}^{T} E_{i,t}^{sell} \times S_{i,t}^{price} \right) \tag{3.6}$$

Here, AEC_{bat} is the annual equivalent cost of battery, integer variable x_{bat} represents the number of the battery modules purchased, $P_{i,t}^{grid}$ and variable $E_{i,t}^{grid}$ represent the external grid price and consumed external grid energy in house i in time t respectively, and finally parameter $S_{i,t}^{price}$ and variable E_{j}^{sell} represent wholesale price and quantity sold to market.

Renewable energy usage The outcome of the first stage calculation is the optimized generation portfolio. Consequently, E_t^{wind}, defined as the total renewable generation from the selected portfolio, serves as an input parameter for the second stage model considered here. Specifically, E_t^{wind} defines the amount of power that can be used for satisfying demand ($E_{i,t}^{rewH}$), charging the battery (E_t^{chr}) and selling on the market (E_t^{sell}). The following constraint expresses this requirement.

$$E_t^{wind} = \sum_{i=1}^{I} E_{i,t}^{rewH} + E_t^{chr} + E_t^{sell} \tag{3.7}$$

Balancing demand The demand is satisfied by wind energy generated ($E_{i,t}^{rewH}$), the energy discharged from the battery ($E_{i,t}^{dchr}$) and the external grid energy purchased ($E_{i,t}^{grid}$) at time t, as given in (3.8). Parameter INV^{rate} corresponds to to the inverter efficiency.

$$D_{i,t}^{house} = (E_{i,t}^{rewH} + E_{i,t}^{dchr}) \times INV^{rate} + E_{i,t}^{grid} \tag{3.8}$$

Foretasted market sales For the operational level problem considered here, we assume that the decision maker has the day-ahead foretasted renewable energy production available, and hence, we assume that the amount that can be sold on the market, that has to be committed in advance, is limited by the foretasted surplus. Consequently, we define E_t^{limit} as the difference between the expected renewable generation and demand, as the upper limit on the amount that can be sold to the external grid the day of generation. Note that here we assume that demand is known a priory in order to concentrate on the uncertainty due to renewable generation (and hence the effect of reducing forecasting error). We define E_t^{limit} = $\max\{$foretasted generation$_t$ $-$ demand$_t, 0\}$, where foretasted generation$_t$ $= \sum_i^n F_i x_i$ and then consider constraint

$$E_t^{sell} \leq E_t^{limit}. \tag{3.9}$$

Battery charge/discharge constraint We define constraints describing the battery dynamics following [59]. Specifically, these ensure balancing the state of charge, that the state of charge is within specified limits and that battery is not charged and discharged at the same time.

$$E_t^{bat} = E_{t-1}^{bat} \times (1 - dchr^{rate}) + E_t^{chr} \times chr^{rate} - \sum_{i=1}^{I} E_{i,t}^{dchr} \tag{3.10}$$

$$SOC^{min} \times C^{bat} \times x_{bat} \leq E_t^{bat} \leq SOC^{max} \times C^{bat} \times x_{bat} \tag{3.11}$$

$$y_t^{chr} + y_t^{dchr} \leq 1 \tag{3.12}$$

$$E_t^{chr} \leq capa^{chr} \times y_t^{chr} \tag{3.13}$$

$$\sum_{t=1}^{T} E_{i,t}^{dchr} \leq capa^{dchr} \times y_t^{dchr} \tag{3.14}$$

$$x_{bat}, E_{i,t}^{grid}, E_{i,t}^{sell}, E_{i,t}^{rew}, E_t^{chr}, E_{i,t}^{dchr}, E_t^{bat} \geq 0 \quad \forall i, t \tag{3.15}$$

$$y_t^{chr}, y_t^{dchr} \in 0, 1 \quad \forall t \tag{3.16}$$

3.4 Case study data

3.4.1 Wind generation profile

We have selected two states as the basis for the numerical experiments. California is selected as a representative example of an area that is suitable for both on- and off-shore wind energy generation. We also select Wyoming, since it has potential to serve as a source for exported wind energy, as it has significant wind energy reserves and relatively low in-state demand. Figure 3.4 shows randomly selected wind sites in each state. Note that we chose not to use all of the locations for the sake of computational tractability. Instead, we sample from the list of the available sites so that the resulting generation locations are distributed across the whole state as uniformly as possible.

We use the actual and forecasted (day ahead) wind generation data provided by National Renewable Energy Laboratory (NREL) through DR POWER dataset ([35]). The database provides observations on actual and forecasted wind energy generation for wind sites in the U.S. The data is derived from the Wind Integration National Dataset (WIND) Toolkit ([52]).

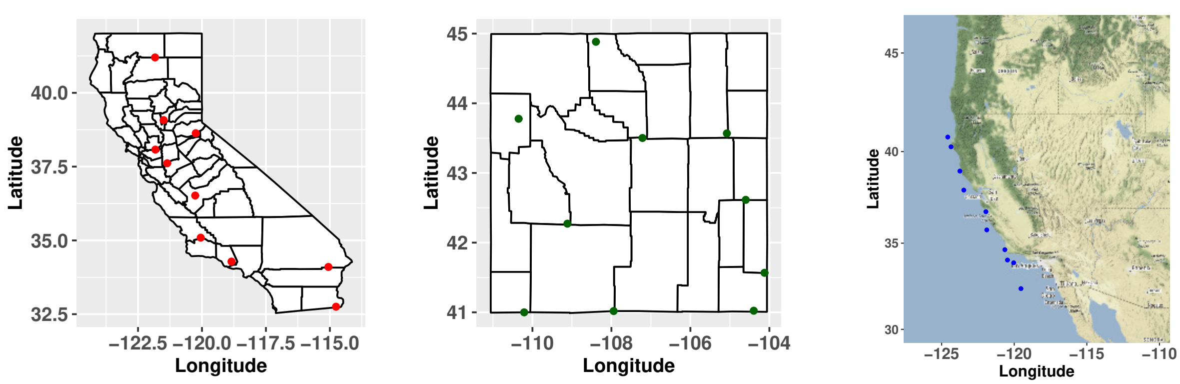

(a) California (CA) **(b)** Wyoming (WY) **(c)** Offshore (CA)

Figure 3.4: Generation sites used in the study.

3.4.2 Demand data

Since the selected generation cites correspond to California and Wyoming, we try to define demand profile as representing the typical residential demand from the two states. Specifically, we assume that the microgrid in question consists of the equal number of typical houses from either of the states, such that the average demand for each house is consistent with the 2019 Average Monthly Bill (Residential) [60]. Further, we scale the total demand in such a way that the average total demand is equal to the average generation from a single wind facility given in the NREL dataset (i.e., on average the demand of the selected microgrid can be matched by the average wind generation) by increasing the number of typical houses used. Table 3.2 provides the resulting values. Finally, in order to reflect the seasonality in the energy demand, we apply the seasonal pattern extracted from the historical grid-level demand data of the corresponding operator (CISO for CA and PACE for WY) [72]. Figure 3.5 presents the resulting demand profile used in the case study accounting for the seasonal factors.

State	Average consumption(Kw/h)	Number of households	Total energy consumption(Kw/h)
CA	17.7	116	3340.8
WY	28.8	116	2053.2

Table 3.2: Sumamry of demand parameters

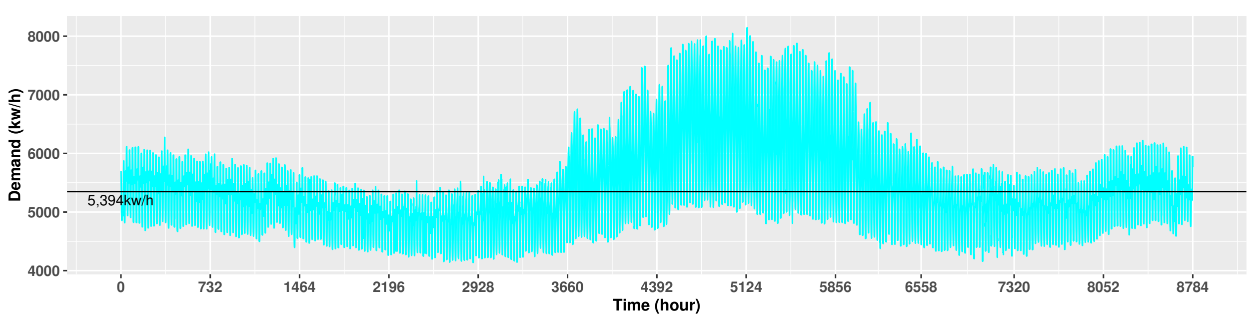

(a) Total Households demand

Figure 3.5: Normalized household demand profile used in the case study.

3.4.3 Battery data

Storage units used for the model are assumed to be household batteries with parameters as described in [70]. The specifications are listed in Table 3.3.

Parameter	Value	Description
AEC^{bat}	269.57(USD)	AEC of single battery module
$Capa^{bat}$	3.3(kwh)	Capacity of single battery module
SOC^{min}	5%	Minimum state of charge
SOC^{max}	95%	Maximum state of charge
chr^{rate}	99%	Charging efficiency
$dchr^{rate}$	0.139%	Self-discharging efficiency
$capa^{chr}$	51%	Maximum charging power
$capa^{dchr}$	51%	Maximum discharging power
IOC	30%	Initial SOC in the battery

Table 3.3: Assumed battery specifications.

3.4.4 Grid and market price

To simplify the model and concentrate on the effect of pooling renewable resources, we assume constant sale and purchasing market electricity prices. For the purchasing price we use the average grid price for each state, following [60]. The wholesale price used is the average wholesale price of wind energy to market according to [73]. The values are reported in Table 3.4. Note that due to the price structure assumption, the microgrid cannot benefit from buying external energy during low-cost periods to store and then sell it during high-cost periods, i.e., any benefit from storage is due to the ability to use more renewable energy.

Parameter	Value	Description
$P^{grid}_{i,t}$	WY: 11.18(cent)	Average grid price in Wyoming state
	CA: 19.15(cent)	Average grid price in California state
S^{price}	1.3(cent)	Average wholesale price of wind energy to market

Table 3.4: Summary of assumed market prices.

3.5 Results of the case study and discussion

Table 3.5 summarizes the scenarios used in the case study to investigate the proposed effect of pooling. Specifically, we consider four pooling cases (no pooling, on-shore, off-shore, and combined). For each onshore case, we separately consider each of the two individual states and the two states together. Finally, in each case, we also consider two operation versions: as a grid-connected or grid-disconnected cases. In the no-pooling case we consider generation from each individual location separately, and then report the results averaged over all sites.

Pooling case	Symbol	Location	Operation scenario
No pooling	Onshore(No pooling)	California, Wyoming	Connected / Disconnected grid
	Offshore(No pooling)	Offshore	Connected / Disconnected grid
Onshore	Onshore(CA)	California	Connected / Disconnected grid
	Onshore(WY)	Wyoming	Connected / Disconnected grid
	Onshore(both)	California, Wyoming	Connected / Disconnected grid
Offshore	Offshore	Offshore	Connected / Disconnected grid
Combined	Combined	California, Wyoming, Offshore	Connected / Disconnected grid

Table 3.5: Case study scenarios.

All underlying optimization problems are solved with Pyomo version 6.2 ([74]) with Gurobi version 9.0, on a desktop computer with an Intel Core i5 processor and 8GB of RAM. Each scenario approximately takes 1 hour to obtain the solution.

3.5.1 Results for grid-connected operation scenarios

First, we consider the model under all pooling cases in the grid-connected operation scenario. In addition, we also consider three levels for the battery cost in order to investigate the sensitivity of the model to this parameter. We set the battery cost following scenarios identified by National Renewable Energy Laboratory (defined as high, mid, and low) for battery cost reduction through 2030 and 2050 [75], which results in the values used.

Battery cost	Pooling	Battery module	Discharge energy (Kw)	Charge energy (Kw)	SOC deviation
$269.57	Combined	1	794.84	803.20	27.56
	Onshore(No Pooling)	1274.65	503,506.16	512,150.48	25.39
	Onshore(CA)	1	1,112.42	1,124.14	30.86
	Onshore(WY)	1	1,201.12	1,213.67	28.27
	Onshore(Both)	1	971.36	981.55	28.23
	Offshore(No Pooling)	1.1	606.79	613.12	15.27
	Offshore	1	729.76	737.39	25.23
$99.74	Combined	1	797.12	805.51	27.58
	Onshore(No Pooling)	1578.55	811,734.28	823,843.39	26.51
	Onshore(CA)	321	304,372.68	307,795.48	30.60
	Onshore(WY)	179	184,627.14	186,659.51	28.07
	Onshore(Both)	66	60,258.06	60,925.18	28.29
	Offshore(No Pooling)	72.1	64,226.91	64,939.08	19.53
	Offshore	1	729.50	737.13	25.23
$59.30	Combined	341	219641.20	222,175.30	27.56
	Onshore(No Pooling)	1955.15	1034465.16	1,049,326.62	26.58
	Onshore(CA)	930	710861.50	719,171.00	30.86
	Onshore(WY)	533	404365.90	409,007.40	28.27
	Onshore(Both)	526	373435.30	377,744.30	28.23
	Offshore(No Pooling)	302.9	199266.76	201,584.10	24.38
	Offshore	172	106025.40	107235.80	25.23

Battery cost	Pooling	Total Cost (cent)	Used Renewable energy (Kw)	Used Grid energy (Kw)	Selling energy (Kw)
$269.57	Combined	91,501,471	39,080,189	9,081,532	10,103,789
	Onshore(No Pooling)	302,445,910	25,311,475	22,082,214	22,168,604
	Onshore(CA)	132,335,747	35,930,754	12,167,667	11,432,592
	Onshore(WY)	126,552,166	36,318,980	11,787,119	13,936,821
	Onshore(Both)	94,814,600	38,956,464	9,202,610	9,989,876
	Offshore(No Pooling)	236,839,246	27,574,825	20,356,973	28,336,193
	Offshore	129,458,254	35,834,465	12,262,405	15,471,024
$99.74	Combined	91,484,468	39,080,189	9,081,530	10,103,787
	Onshore(No Pooling)	279,614,500	25,259,180	21,831,400	21,909,207
	Onshore(CA)	131,776,775	35,895,011	11,905,500	11,161,664
	Onshore(WY)	126,218,738	36,281,606	11,643,988	13,788,748
	Onshore(Both)	94,759,229	38,949,236	9,151,592	9,937,160
	Offshore(No Pooling)	236,708,125	27,556,572	20,312,513	28,290,120
	Offshore	129,441,274	35,834,465	12,262,405	15,471,024
$59.30	Combined	91,202,053	39,045,868	8,900,697	9,916,738
	Onshore(No Pooling)	272,597,194	25,243,618	21,628,375	21,699,286
	Onshore(CA)	129,573,147	35,887,330	11,514,668	10,757,969
	Onshore(WY)	124,991,661	36,257,744	11,452,029	13,590,263
	Onshore(Both)	93,720,405	38,916,962	8,876,307	9,652,615
	Offshore(No Pooling)	236,005,146	27,530,263	20,205,957	28,179,784
	Offshore	129,304,013	35,804,454	12,188,626	15,394,537

Table 3.6: Results of the base case of the case study.

Table 3.6 summarises the main results. Here we report the summary of the performance of the system, as well as relevant costs. Specifically, we report: number of battery units purchased, total charge and discharge energy, SOC (State of Charge) deviation defined a variability of battery energy for period, total system cost, amount of each source of energy used (renewables vs grid) and amount of energy sold on the market. Note that in the case of no-pooling, the reported results are averaged between each of the individual generation locations.

First, observe that in all cases either the combined pooling or onshore (both) scenario achieves the lowest operational cost, the highest level of renewable energy use, and the lowest level of grid energy used. Naturally, these three metrics are directly related, since, as defined, renewable generation is free (i.e., the cost is fixed), and hence higher use of renewables (lower grid use) directly translates into the lower total cost. In most cases, the combined pooling case outperforms the onshore only case. Both significantly outperform pooling cases, when the two states are separated, as well as off-shore only cases. Most importantly, all pooled portfolios result is substantially lower costs compared to no pooling cases (up to two times). We can also observe that pooling renewable energy results in a significant reduction in the need for energy storage. For example, for the low-cost case, pooling generation across onshore locations in CA results in 54% reduction in battery units, and 72% reduction in case of WY. Note that this reduction is accompanied by the significant increase in the use of renewable generation (as opposed to grid energy), and hence directly translates into lowering emissions both during generation and battery unit production (since fewer batteries are needed). Interestingly, the change in battery cost, while having a significant effect on the number of units used, does not have a large effect on the total cost. The conclusions are further supported by Figure 3.6, which depicts the relative proportion of renewable vs grid energy used in each scenario. Here we can observe that the batteries, while employed to some extent, in fact did not play a substantial role in the system, i.e., most of the benefits in this case follow directly from the reduction in forecasting error and/or intermittency. Overall, we can conclude that pooling geographically diverse wind generation can significantly reduce the dependence of the external grid.

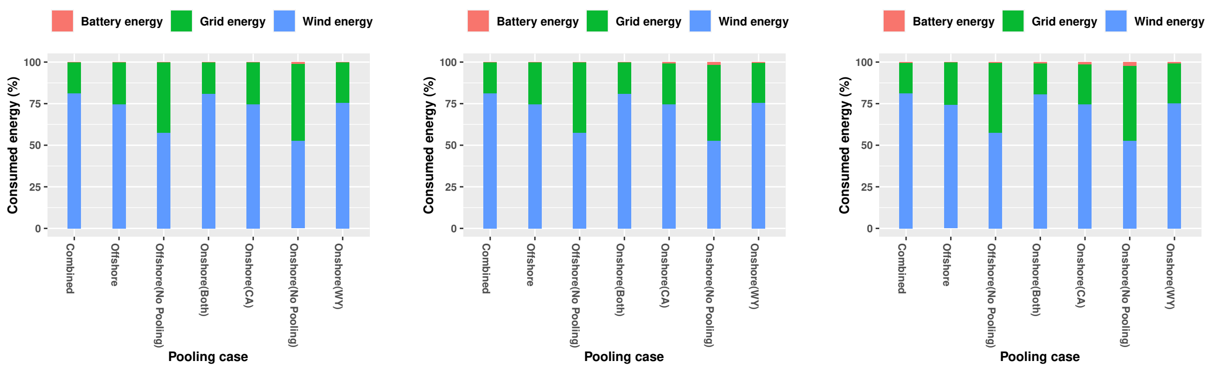

(a) Battery Cost: $269.57 **(b)** Battery Cost: $99.74 **(c)** Battery Cost: $59.30

Figure 3.6: Energy sources by type for each of the portfolios.

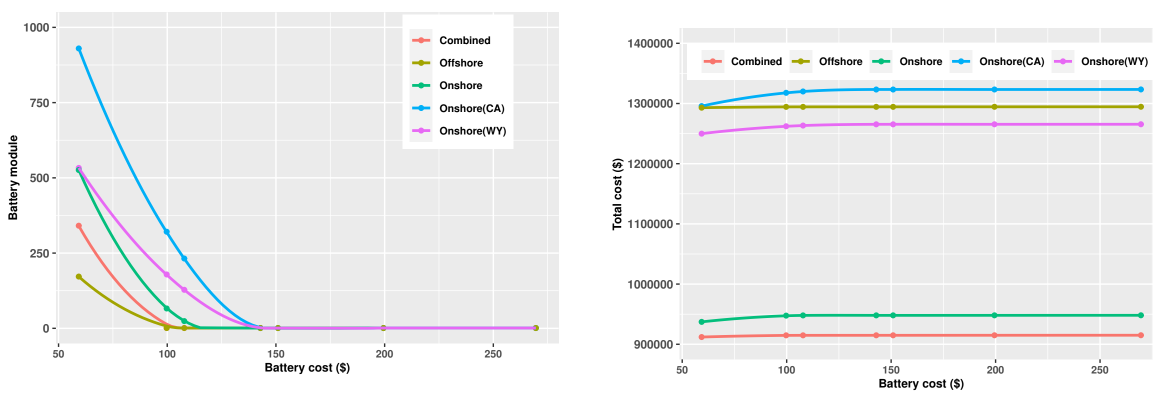

(a) The number of Battery module changes by pooling case

(b) The total cost changes by pooling case

Figure 3.7: Result of the sensitivity analysis with respect to battery cost.

Focusing on the effect of battery cost, Figures 3.7 and 3.7a depict the change in the number of units purchased as well as total cost in each scenario as a function of unit cost. Once again observe that the pooling over large region (i.e., combined pooling vs onshore over both states, vs offshore or onshore separated by state) is significantly more efficient. The cost of a battery has a large effect on the number of units used and a smaller effect on increasing the total cost.

3.5.2 Result of grid-disconnected operation scenario

Next, we consider the grid-disconnected case. Naturally, in this case, it may be impossible to meet the demand with renewable generation only given the way that the experiment is set up. To account for this, we assume infinite battery capacity. We also report the amount of unmet demand, which serves as the primary comparison criterion in this case.

Table 3.7 and Figure 3.8 summarize the results in this case. As before, in this case, more efficient pooling directly translates into improved solutions, both in terms of cost and unmet demand, i.e., combined pooling portfolios result in lower cost and less unmet demand, compared to single-state pooled cases (or off-shore only), which in turn, outperform no-pooling cases.

Pooling	Total Cost(cent)	Discharge energy(kw)	Selling energy(kw)	Total unmet demand quantity(kw)
Combined	249,902,241	335,967	9,763,031	8,752,940
Onshore(No pooling)	643,213,094	142,225	22,515,343	22,415,902
Onshore(CA)	342,256,062	282,865	11,147,216	11,891,382
Onshore(WY)	328,011,366	267,635	13,666,614	11,525,733
Onshore(Both)	254,313,217	313,647	9,672,881	8,896,066
Offshore(No pooling)	572,062,164	64,987	28,270,583	20,293,698
Offshore	340,535,311	258,002	15,209,231	12,010,044

Table 3.7: Results for the grid-disconnected case.

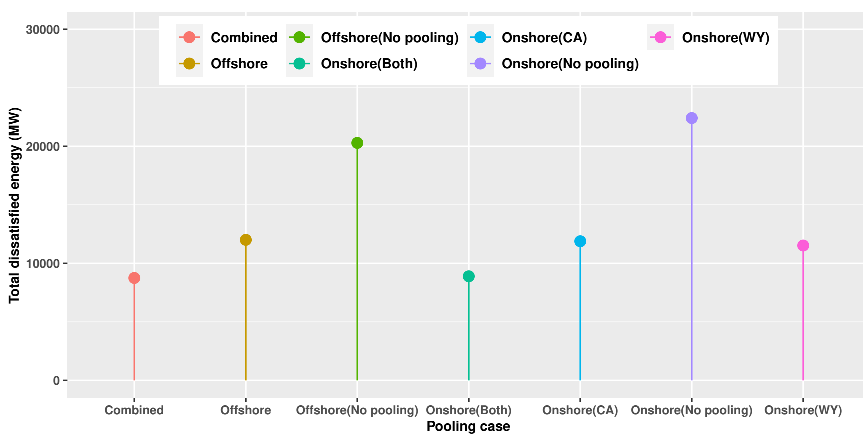

Figure 3.8: Total dissatisfied energy in the grid disconnected case by portfolio type.

3.5.3 Effect of demand on grid-connected operation scenario

In addition, we also consider the effect of demand level. Specifically, we consider four cases with different average demand levels, corresponding to up to 30% change compared to the base case. Figures 3.9 and 3.9a summarize the results comparing the four demand levels and five pooled portfolios. Naturally, higher demand results in more battery requirements and higher costs. Note though, that most importantly for our purposes, the relative performance of the portfolios by pooling type does not change, i.e., we can conclude that the observations made above do not seem to be significantly sensitive to demand level.

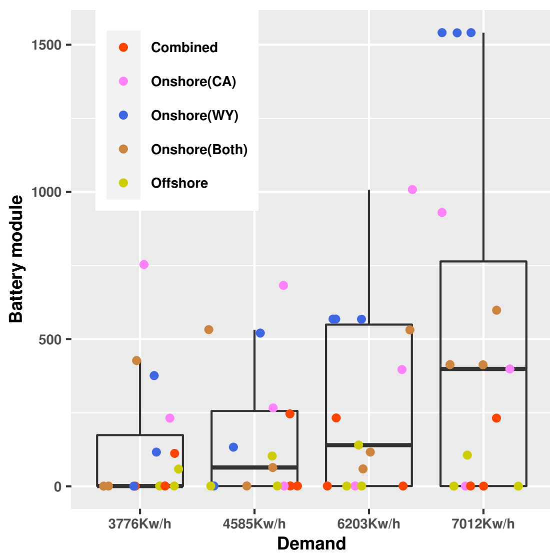

(a) number of battery modules required

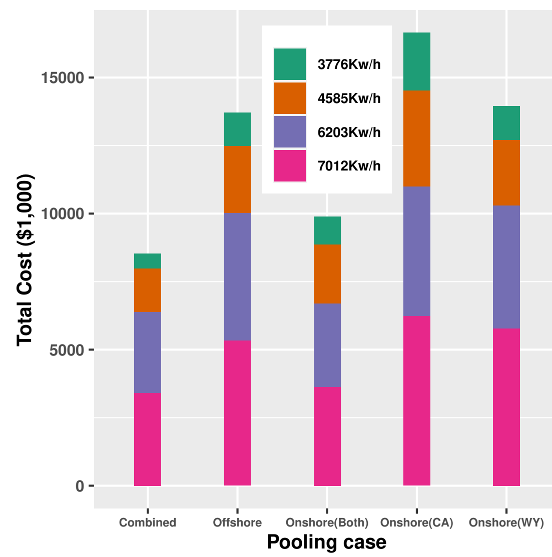

(b) total cost

Figure 3.9: Result of sensitivity analysis with respect to demand level.

3.6 Conclusion

The study proposes a heuristic approach aimed at simultaneous optimization of wind energy portfolio (to reduce variability) and battery requirenment/operational costs in a microgrid. Specifically, we investigate whether the benefits identified in the previous effort (reduction in variability) will translate into a reduction of operational costs in capital investment problems, e.g., a battery sizing problem. A heuristic approach to the two-stage sizing problem is constructed. A mean-CVaR optimization model provides a family of optimal generation portfolios for a pre-determined harvesting region based on real data from US states, which is designed to take advantage of the correlation structure in the generation and forecasting profiles in order to reduce the overall error while maintaining satisfactory expected generation. Next, the operation planning model optimizes the assignment of wind , battery and grid energy to achieve the demand load. We evaluate the pooling effect on the battery size and total cost in different scenarios such as geographically and/or technologically diverse wind generation locations.

Most importantly, the results have shown that pooled portfolios always outperform no-pooling case. More specifically, if the generation capacity is optimally spread over a single state, it can lead to lower operational cost and lower storage requirement, compared to a microgrid power by generation from a single location. Further, if generation can be spread across multiple states and/or includes both on- and off-shore sites, it further significantly increases system efficiency. For example, geographically pooling in California only can result in 52% reduction in battery modules needed, as well as 52% reduction in the total cost compared to no pooling cases. It is important that our approach can achieve a significant pooling effect even in the same interconnect area already constructed transmission network. Polling across both CA and WY and off-shore locations further reduce the numbers by 73%, 91% reduction in battery module needed, as well as 66%, 53% reduction in the total cost respectively compared to no pooling cases.

The outcomes of the sensitivity analysis serve to highlight the robustness of the observed results in the base case. Specifically, pooling significantly reduces the battery requirement and the total cost in all tested scenarios, including different battery cost and demand levels as well as grid-connected or grid-disconnected cases. Similarly, pooling across multiple states and including both on- and off-shore sources further reduce the incurred operational costs. Consequently, we conclude that, whenever possible, intelligent planning for pooling geographically diverse renewable energy sources can serve as an important tool for overcoming generation variability challenges.

A number of limitations and directions for future research of the study must be emphasized. First, we did not consider the transmission cost in geographical pooling. The cost of energy being transported through the different regions is clearly one of the operating costs that would reduce the realized benefits. Secondly, the obtained operation planning results may not be optimized since we evaluated the effect of pooling on battery sizing through operation plans. It is necessary to optimize the results and operational planning of pooling together with the multi-stage model in future work.

Chapter 4

Multilevel modeling with risk-averse model for renewable energy management in virtual power plant

4.1 Introduction

Renewable energy systems are projected to observe rapid development through distribution, networking, and intelligence [76, 77]. The high permeability of renewable energy requires integration of information and energy flows, which provides advantages such as flexibility of power systems without further investment in infrastructure [78]. Virtual power plants (VPPs) are one of the important technologies to balance grids with renewable generators and make smart grid distribution networks more intelligent [79] compared to conventional microgrid. It has the capabilities of heterogeneous distributed energy resources (DER) to increase power generation, as well as to trade or sell electricity on an open market [80].

As a result, this work focuses on modeling for simultaneous optimization of wind energy portfolios related to geographically pooling wind energy sources and energy management planning in smart grid systems with VPPs. Note that operation planning model is focused on ancillary services such as reserve energy, selling energy instead of battery capacity, as was the case in the previous chapter since it is a critical role of VPPS to control the distributed sources. In other words, we make the model more comprehensive by allowing to optimize over both operation planning and portfolio at the same time while the previous chapter 3 optimizes the wind energy portfolio and operation planning (focused on battery capacity) separately. To this end, we propose multilevel modeling to optimize risk-averse portfolio and operation planning for energy management. Specifically, the same mechanism that results in a reduction in intermittency instead of forecasting error with geographical pooling also applies to the current risk-averse portfolio at the first level [15]. Moreover, the optimal portfolios obtained by risk-averse portfolios can be adjusted to optimize the operation planning at the second level. Most importantly, it is clear that by applying multilevel modeling it may be possible to further improve on energy management.

Moreover, we investigate the effect of multilevel modeling on operation planning compared to a heuristic approach considered in the previous chapter. We also broadly examine the effect of geographical pooling on the multilevel model and change to the variable in the model such as battery capacity, risk tolerance, and reserve energy cost. Consequently, the goal of this effort is to consider the following three research questions:

- What is the impact of multilevel modeling in energy management in different areas and achieving coordinated energy generation;
- To what extent is it possible to increase the reliability for VPPs by pooling together geographically diverse sources;
- How much cost can be reduced in the smart grid through the multilevel modeling;

To this end, we design a simulation study, based on historical wind generation data (day-ahead forecast) for the State of California. This chapter again uses risk-averse portfolio optimization with Conditional-Value-at-Risk (CVaR) as the underlying pooling technique due to its popularity in stochastic optimization research. We also use a linear programming model for operation planning in multilevel modeling. Three months' worth of historical observations (Winter, Summer) is used to construct a collection of optimized wind generation portfolios, and then evaluate its performance in terms of total operating cost in a smart grid for a series of test regions, ranging from county-level to state-level.

The contributions of the effort are as follows. First, this paper proposes a multilevel model for designing a wind energy portfolio and optimization of operation planning, with the goal of minimizing the total operation cost in smart grid associated with intermittency (measured by CVaR) and while ensuring satisfactory demand load. Secondly, by applying the multilevel model in a case study, it can be observed that the total operation cost in a smart grid can be significantly decreased compared to a benchmark (heuristic approach). We observe that, while it is possible to reduce the operation cost by a heuristic approach that represented optimizing wind energy portfolio and operation planning separately instead of multilevel modeling, employing a multilevel model allows for better renewable management. Finally, this study obtain the result that the scale of this improvement depends on the size of the harvesting area.

The remainder of the chapter is organized as follows. Section 4.2 provides a problem description. Section 4.3 presents the proposed multilevel model with mathematical formulation and the corresponding methodology used to organize the case study. Section 4.4 describes a scenario of case study and system data for simulation. Section 4.5 discusses the results of the case study. Finally, Section 4.6 concludes the discussion and outlines some ideas for future research.

4.2 Description of smart grid system

Figure 4.1 describes the overall scheme of the smart grid system, which is generally similar to the one used in the previous chapter. We assume that a virtual power plant management system is connected with a number of wind facilities (onshore) as integrated renewable sources, storage, and markets to sell/purchase the energy for balancing with demand. We also assumed the wind energy is consumed by a set of households. See more details in section 3.2.

At the same time, it is worth emphasizing that the reserve energy is used to supply the extra energy to achieve the demand under uncertainty. Specifically, the reserve energy is prepared to reduce optimal operation planning and system costs by supplementing the optimal portfolio through limited predictive capabilities [81]. Reserve energy is an efficient means of supplementing energy intermittency. We assume that there are two types of reserve energy (reserve, emergency reserve). Furthermore, the emergency reserve energy is only used for the situation that the system can not achieve the household demand. Moreover, too much reserve energy can affect the capacity of the energy system and makes the energy system uneconomical. At the same time, too small reserve energy may not meet uncertain demand, resulting in loss of energy cost. Therefore, a virtual power plant management system simultaneously optimize wind facilities portfolio and operation planning (battery energy, selling energy, reserve energy).

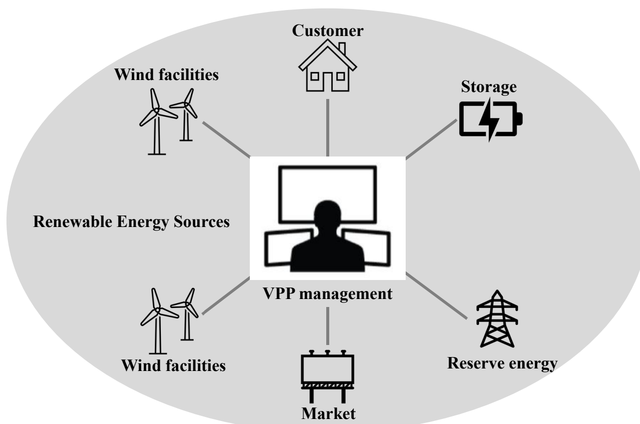

Figure 4.1: Virtual Power Plant scheme

4.3 Research methodology

The study proposes a multilevel optimization problem to allow to optimize over both operation and portfolio at the same time. It is noted that multilevel optimization problems are mathematical programs that have a subset of their variables constrained to be an optimal solution of other programs parameterized by their remaining variables [82, 83]. Figure 4.2 describes a problem-solving approach for a multilevel model with a mean-CVaR model. In detail, in the first level, we derive optimal wind energy portfolios from a risk-averse optimization model. At the second level, we

Indices		Variables	
h	house (h = 1...H)	E_t^{res}	reserve energy during period t (kwh)
t	time (t = 1...T)	E_t^{wind}	wind energy output during period t (kwh)
i	facility (i = 1...I)	$E_{h,t}^{rewH}$	used wind energy in house h during period t (kwh)
j	scenario (j = 1...J)	$E_t^{reserve}$	total expected reserve energy during period t(kwh)
		$E_{h,t}^{resH}$	used reserve energy in house h during period t (kwh)
Parameters		$E_{h,t}^{em}$	used emergency reserve energy in house h during period t (kwh)
d_o	expected average demand load per hour	E_t^{sell}	selling wind energy during period t (kwh)
$\bar{F}_i$	average forcasted generation in facility i	E_t^{chr}	charge energy in the batter during period t (kwh)
x_{bat}	number of the battery	$E_{h,t}^{dchr}$	discharge energy in the batter to house h during period t (kwh)
P^{res}	price of reserve energy	E_t^{bat}	available energy in the battery during period t (kwh)
P_t^{em}	emergency reserve cost during period t (cent)	y_t^{chr}	binary variable variable to indicate charging state during t
P_t^{sell}	wholesale wind energy price during period t (cent)	y_t^{dchr}	binary variable variable to indicate discharging state during t
$D_{i,t}^{house}$	energy consumption in house i during period t (kwh)	x_i	optimal investment level at facility i
INV^{rate}	invereter efficiency (%)	w_j	auxiliary variable
$dchr^{rate}$	self-discharging efficiency (%)}	η	Value at risk (VaR)
chr^{rate}	charging efficiency (%)	u_j	dual variable corresponding to the inequality w_t
C^{bat}	capacity of single battery module (kwh)	u_0	dual variable target equation A_0
$capa^{chr}$	maximum charging power (%)	ξ	Dual variable corresponding to the budget equation
$capa^{dchr}$	maximum discharging power (%)		
IOC	initial SOC in the battery (%)		
SOC^{min}	minimum state of charge (%)		
SOC^{max}	maximum state of charge (%)		

Table 4.1: Nomenclature used

optimize operation planning (reserve energy, battery energy, selling energy) by adjusting the optimal wind portfolio simultaneously. It is worth emphasizing that this approach is different from the previous heuristic approach whereby the stages are separated and solved one after the other.

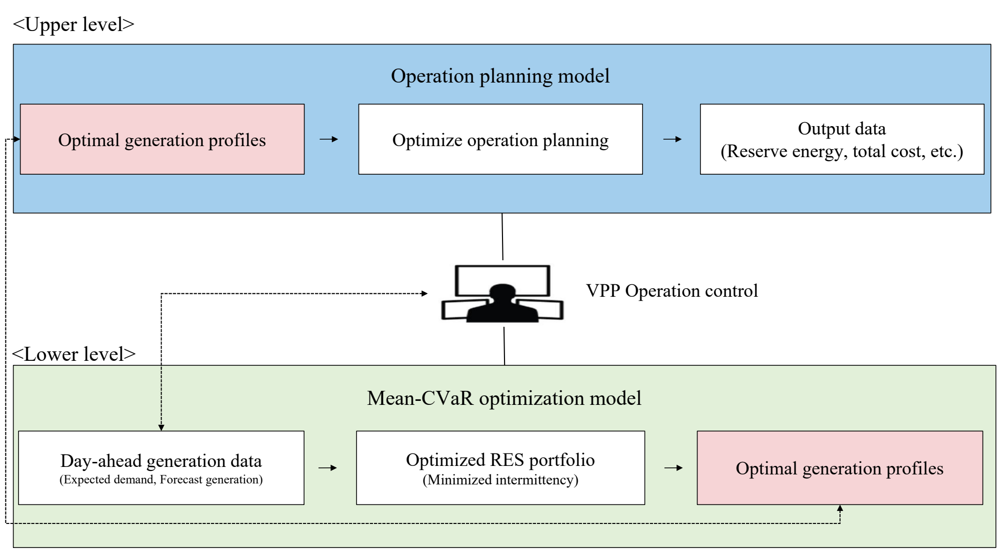

Figure 4.2: Proposed optimization framework.

4.3.1 Mean-CVaR model

At the first level (lower level), our portfolio construction methodology is based on risk-averse stochastic optimization, Mean-Conditional Value-at-Risk (Mean-CVaR). In formulating this problem we follow the standard approach used in CVaR optimization.

Primal model We consider a portfolio optimization model, aimed at minimizing the risk (as measured by CVaR) of underproduction subject to budget constraints by pooling n pre-identified potential generation sites, with underproduction defined as $\ell = max\{\mathbf{d} - \mathbf{F}^{\mathsf{T}}\mathbf{x}, 0\}$. In other words, our model tries to minimize the difference between demand and forecasted generation. We define as $\mathbf{F_i}$ the vectors representing day-ahead forecasted generation from the selected sites. F_{ij} gives the forecasted generation at site i under scenario j. We assume that there are n candidate locations and m historical scenarios based on seasonality. Finally, the underlying portfolio design optimization problem Eq. (4.1) – (4.5) can be formulated as a linear program (LP) as follows and see all detail of equation and parameter value in previous chapter 2.

$$\min_{\eta\in\mathbb{R},\mathbf{w}\in\mathbb{R}^m,\mathbf{x}\in\mathbb{R}^n} \quad \eta + \frac{1}{(1-\alpha)m}\sum_{j}^{m} w_j \tag{4.1}$$

$$\sum_{i}^{n} x_i = 1 \tag{4.2}$$

$$\sum_{i}^{n} \bar{F}_i x_i \geq A_o \tag{4.3}$$

$$w_j \geq (d_o - \sum_{i=1}^{n} F_{ij} x_i) - \eta \tag{4.4}$$

$$x, w \geq 0 \tag{4.5}$$

Dual model To enable an exact solution to the bi-level problem, we will employ the dual model based on the strong duality [84]. For more context in formulating dual problems for CVaR optimization, see [85]. A dual model for the CVaR portfolio optimization problem above can be formulated as follows.

$$\max_{\xi, u_0} \quad \xi + A_0 u_0 \tag{4.6}$$

$$\xi + \bar{A}_i u_0 + (d_o - \sum_{j=1}^{J} F_{ij} u_j) \leq 0 \tag{4.7}$$

$$\sum_{j}^{J} u_j = 1 \tag{4.8}$$

$$u_j \leq \frac{1}{(1-\alpha)m} \tag{4.9}$$

$$u \geq 0 \tag{4.10}$$

Here, dual variable ξ corresponds to the primal Eq. (4.1), variable u_0 corresponds to the inequality primal constraint Eq. (4.2), and u_j corresponds to inequality (4.3).

4.3.2 Operation planning model

At the second level (upper level), the operational planning model provides the interaction between the selected generation portfolio and operation planning. Specifically, the decision-making problem here is to minimize the total cost (due to reserve, battery and market interaction) given the realized renewable generation. The model is a binary (linear) optimization problem and given in Eq.(4.11) – (4.23).

$$\min \quad \sum_{h=1}^{H}\sum_{t=1}^{T} E_{h,t}^{em} \times P^{em} + \sum_{t=1}^{T} E_t^{reserved} \times P^{res} - \sum_{t=1}^{T} E_t^{sell} \times P_t^{sell} \tag{4.11}$$

$$E_t^{wind} = \sum_{i=1}^{n} F_{ij} \times x_i \tag{4.12}$$

$$E_t^{reserved} = \left| d_o - \sum_{i=1}^{n}(F_{ij}x_i) \right| \tag{4.13}$$

$$E_t^{wind} = \sum_{h=1}^{H} E_{h,t}^{rewH} + E_t^{chr} + E_t^{unused} \tag{4.14}$$

$$E_t^{reserved} = \sum_{h=1}^{H} E_{h,t}^{resH} + E_t^{chr} + E_t^{unused} \tag{4.15}$$

$$D_{h,t}^{house} = (E_{h,t}^{rewH} + E_{h,t}^{resH} + E_{h,t}^{em} + E_{h,t}^{dchr}) \times INV^{rate} \tag{4.16}$$

$$E_t^{bat} = E_{t-1}^{bat} \times (1 - dchr^{rate}) + E_t^{chr} \times chr^{rate} - \sum_{h=1}^{H} E_{h,t}^{dchr} \tag{4.17}$$

$$SOC_{min} * C^{bat} \times x_{bat} \leq E_t^{bat} \leq SOC_{max} \times C^{bat} \times x_{bat} \tag{4.18}$$

$$y_t^{chr} + y_t^{dchr} \leq 1 \tag{4.19}$$

$$E_t^{chr} \leq capa^{chr} \times y_t^{chr} \tag{4.20}$$

$$\sum_{t=1}^{T} E_{h,t}^{dchr} \leq capa^{dchr} \times y_t^{dchr} \tag{4.21}$$

$$E_{h,t}^{em}, E_t^{reserved}, E_{h,t}^{sell}, E_{h,t}^{rew}, E_t^{chr}, E_{h,t}^{dchr}, E_t^{bat} \geq 0 \quad \forall h,t \tag{4.22}$$

$$y_t^{chr}, y_t^{dchr} \in 0,1 \quad \forall t \tag{4.23}$$

In Eq. (4.11), the objective of the model is to minimize the total operation cost. Variable reserve energy($E_t^{reserved}$) and emergency reserve energy ($E_{h,t}^{em}$) ensure that the amount of wind energy is equal to the demand. The price of reserve energy (P^{res}), emergency reserve energy (P^{em}) and selling energy (P_t^{sell}) respectively, are known parameters. Eq. (4.12) calculates the amount of wind energy from the first level model. Eq. (4.13) defines the amount of reserve energy at the optimal portfolio. It is noted that emergency reserve energy is only used in extreme cases where demand cannot be satisfied. Eq. (4.14) – (4.15) represents energy equivalent constraints. Eq. (4.16) ensures that household demands are achieved by wind, battery, and each of the reserves. Eq. (4.17) calculates available energy in the battery. Eq. (4.18) guarantees a durable life of the battery that state of charge(SOC) must be between the minimum and maximum range of SOC. In the Eq. (4.19), the binary variables (y_t^{chr},y_t^{dchr}) prevent charging or discharging simultaneously in the battery. Eq. (4.20) – (4.21) enforced the charged/discharged energy at time t must be less than or equal to the maximum charging/discharging energy capacity ($capa^{chr}$/$capa^{dchr}$). Finally, Eqs. (4.22) – (4.23) restrict seven non-negative continuous variables and two binary variables.

4.3.3 Multilevel model mathematical formulation

By employing optimality conditions we can rewrite the bi-level optimization problem as a single-level LP as follows.

$$\min \quad \sum_{i=1}^{I}\sum_{t=1}^{T} E_{i,t}^{em} \times P^{em} + \sum_{t=1}^{T} E_t^{reserved} \times P^{res} - \sum_{t=1}^{T} E_t^{sell} \times P_t^{sell} \tag{4.24}$$

$$\sum_{i}^{n} x_i = 1 \tag{4.25}$$

$$\sum_{i}^{n} \bar{A}_i x_i \geq A_o \tag{4.26}$$

$$w_j \geq (d_o - \sum_{i=1}^{n} F_{ij} x_i) - \eta \tag{4.27}$$

$$\xi + \bar{A}_i u_0 + (d_o - \sum_{j=1}^{J} F_{ij} u_j) \leq 0 \tag{4.28}$$

$$\sum_{j}^{J} u_j = 1 \tag{4.29}$$

$$u_j \leq \frac{1}{(1-\alpha)m} \tag{4.30}$$

$$\eta + \frac{1}{(1-\alpha)m} \sum_{t}^{m} w_t = \xi + A_0 u_0 \tag{4.31}$$

$$E_t^{wind} = \sum_{i=1}^{n} F_{ij} \times x_i \tag{4.32}$$

$$E_t^{reserved} = \left| d_o - \sum_{i=1}^{n} (F_{ij} x_i) \right| \tag{4.33}$$

$$E_t^{wind} = \sum_{h=1}^{H} E_{h,t}^{rewH} + E_t^{chr} + E_t^{unused} \tag{4.34}$$

$$E_t^{reserved} = \sum_{h=1}^{H} E_{h,t}^{resH} + E_t^{chr} + E_t^{unused} \tag{4.35}$$

$$D_{h,t}^{house} = (E_{h,t}^{rewH} + E_{h,t}^{resH} + E_{h,t}^{em} + E_{h,t}^{dchr}) \times INV^{rate} \tag{4.36}$$

$$E_t^{bat} = E_{t-1}^{bat} \times (1 - dchr^{rate}) + E_t^{chr} \times chr^{rate} - \sum_{h=1}^{H} E_{h,t}^{dchr} \tag{4.37}$$

$$SOC_{min} * C^{bat} \times x_{bat} \leq E_t^{bat} \leq SOC_{max} \times C^{bat} \times x_{bat} \tag{4.38}$$

$$y_t^{chr} + y_t^{dchr} \leq 1 \tag{4.39}$$

$$E_t^{chr} \leq capa^{chr} \times y_t^{chr} \tag{4.40}$$

$$\sum_{t=1}^{T} E_{h,t}^{dchr} \leq capa^{dchr} \times y_t^{dchr} \tag{4.41}$$

$$E_{h,t}^{em}, E_t^{reserved}, E_{h,t}^{sell}, E_{h,t}^{rew}, E_t^{chr}, E_{h,t}^{dchr}, E_t^{bat} \geq 0 \quad \forall h, t \tag{4.42}$$

$$y_t^{chr}, y_t^{dchr} \in 0, 1 \quad \forall t \tag{4.43}$$

$$x, w \geq 0 \tag{4.44}$$

Eq. (4.31) represents primal-dual optimality condition based on strong duality.

4.4 Case study data

4.4.1 Wind generation profile

In order to investigate the model performance, we conduct a series of numerical experiments, using the State of California as the basis. Figure 4.3 demonstrates randomly selected wind sites with regions in the state. In detail, we split the state vertically, creating whole, half, and quarter areas. We then sample from the list of given sites so that the resulting generation sites are distributed across the whole state as uniformly as possible. We obtained historical wind forecast generation data (hourly resolution) provided by National Renewable Energy Laboratory (NREL) from DR POWER ([35]) in the same way as in Chapter 3.

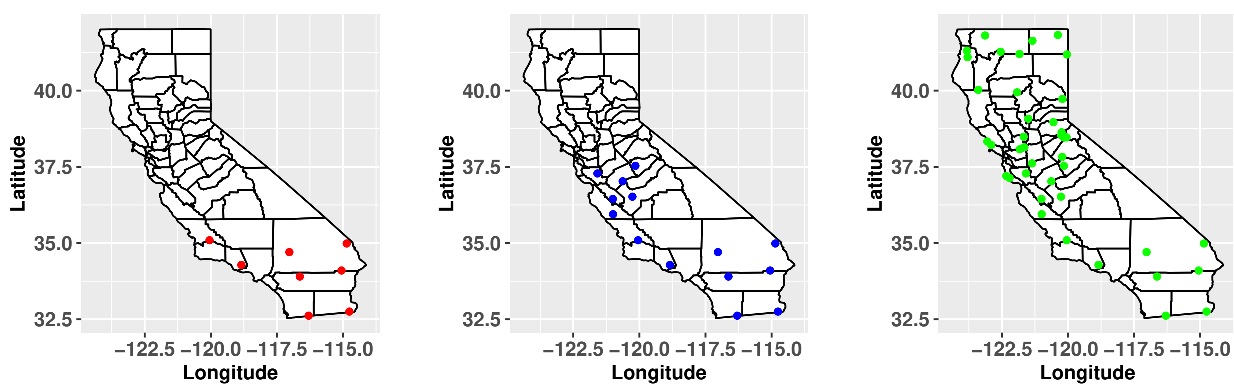

(a) quarter **(b)** Half **(c)** Whole

Figure 4.3: Location of wind generation sites used.

4.4.2 Household demand data

Similarly to the previous chapter (see Section 3.4.2), we try to define demand profile as representing the typical residential demand from the state, on average 17.7 Kw/h per household (2019 Average Monthly Bill for Residents in California [60]) and apply seasonal adjustment. Table 4.2 summarizes relevant demand parameters.

Data	Value	Unit
Average household consumption	17.7	Kw/h
Number of households	232	
Winter average demand	3,820	Kw/h
Summer average demand	4,772	Kw/h

Table 4.2: Assumed demand parameters.

In this chapter we only consider winter (December to February) and summer (June to August) seasons for the case study to reduce the computational burden. The winter and summer periods consist of 2160 and 2208 hours respectively. Figure 4.4 shows the seasonal factor and the variability in each season respectively. Note that household demand is larger in summer than in winter.

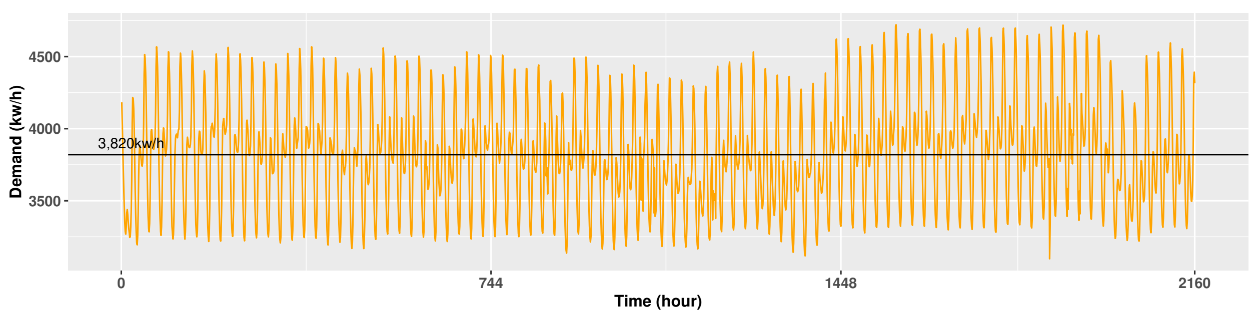

(a) Household Demand in Winter

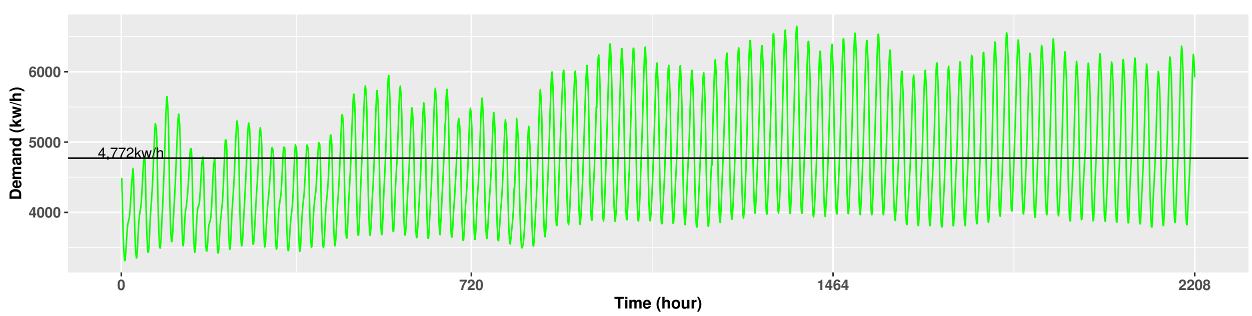

(b) Household Demand in Summer

Figure 4.4: Normalized household demand profile.

4.4.3 Battery data

The battery used for the model is based on LG residential battery which has 3.3 kWh capacity [86]. We assume that the smart grid system has 5 batteries as described in the specification in Table 4.3.

Parameter	Value	Description
$Capa^{bat}$	3.3(Kwh)	Capacity of battery
x_{bat}	5	Total number of battery
SOC^{min}	5%	Minimum state of charge
SOC^{max}	95%	Maximum state of charge
chr^{rate}	99%	Charging efficiency
$dchr^{rate}$	0.139%	Self-discharging efficiency
$capa^{chr}$	51%	Maximum charging power
$capa^{dchr}$	51%	Maximum discharging power
IOC	30%	Initial SOC in the battery

Table 4.3: Assumed battery specifications.

4.4.4 Reserve energy and market price

To define the reserve cost, we assume that it is equal to California grid cost ([60]) as shown in Table 4.4 because one way to purchase it, is from an external grid market [87]. At the same time, we assume that emergency reserve cost is the value of lost load caused by the unbalance with demand load in the smart grid system ([81]). Moreover, we assume constant reserve and emergency reserve costs. Note that these two simplifying assumptions make our model focus on the multilevel model effect, avoiding the confounding effect of reserve energy bid strategy.

Parameter	Value (cent)	Description
$P^{reserve}$	19.15	Average grid price in CA
P^{em}	100,000	Cost for Value of lost load

Table 4.4: Assumed reserve prices.

We also assume that the wholesale price is the average wholesale price (1.3 cents) of wind energy to market according to [73]. We normalized the wholesales (market) price as below Fig 4.5 assuming the standard deviation of 0.3 cents for including the benefit from selling extra energy during high-cost periods instead of storing the energy in the battery.

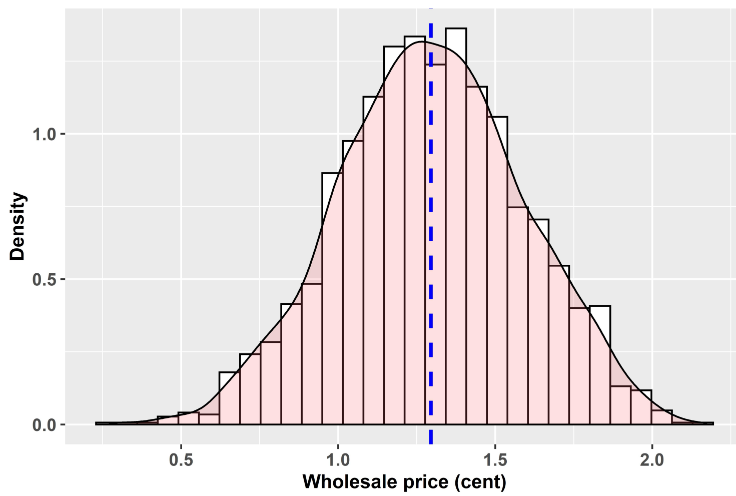

Figure 4.5: Histogram for normalized selling price

4.5 Results of the case study and discussion

Table 4.5 describes the 6 different scenarios denoted according to the season (winter, summer) and pooling region (whole, half, quarter). For example, the winter season in the whole region pooling is denoted as Win-W.

Scenario	Season	Region	Number of Wind facilities
Win-W	Winter	Whole	40
Win-H	Winter	Half	14
Win-Q	Winter	Quarter	8
Sum-W	Summer	Whole	40
Sum-H	Summer	Half	14
Sum-Q	Summer	Quarter	8

Table 4.5: Scenarios used in the case study

The obtained optimal results are compared against the heuristic approach, which was proposed in Chapter 4. It is worth emphasizing that comparing the multilevel model to the heuristic model allows us to evaluate how much operation planning can be improved through optimal pooling by the multilevel method, as opposed to an occurring pooling outcome separately. At the same time, we estimate how the different sizes of RES harvesting regions affect the improvement in operation planning due to pooling. Thus, we conduct a sensitivity analysis of the varied battery capacity, risk tolerance, and reserve energy cost.

All underlying linear programming optimization problems are solved with the optimization package Python Pyomo 6.2 ([74]) with Gurobi version 9.0, on a desktop computer with an Intel Core i5 processor and 32GB of RAM. Each scenario approximately takes 10 minutes to obtain the optimal solution.

4.5.1 Effect of the proposed multilevel model in smart grid system operation

Table 4.6 reports on the performance of the system, as well as relevant costs for the different optimal pooling approaches. We describe total system cost, cost of reserve energy used, and revenue of energy sold on the market. It is noted that we obtained results by separating two seasons in the whole region to account for seasonality.

Season	Methodology	Total cost ($)	Reserve cost ($)	Selling revenue ($)
Winter	Heuristic	- 60,191	32,436	92,627
	Multilevel	- 67,269	30,993	98,262
Summer	Heuristic	54,383	148,492	94,109
	Multilevel	51,623	147,388	95,765

Table 4.6: Case study results for teh base case

First, observe that multilevel model results in smaller total cost compared to heuristic methodology in both seasons. Specifically, in winter it results in 10.5% reduction in total cost, and 5.1%

reduction in summer. While this is not surprising in itself, it is worth emphasizing that the improvement of reserve energy cost and selling revenue compared to heuristic is substantial, with optimization being able to adjust the optimal pooling profile to serve household demand more efficiently. Table B.1 in the Appendix reports the absolute difference (%) of the optimal portfolio by the multilevel model compared to the heuristic approach. Overall, the portfolio difference is affected by seasonality. However, it shows that the multilevel model adjusts optimal pooling results by 34.04% and 2.25% respectively to optimize the operation planning at the second level.

Fig 4.6 compares the generation profiles from each of the individual sites and the two optimal portfolios in terms of the proportion of demand met on average (i.e., the ratio between average generation and demand) and standard deviation. Both optimal portfolios significantly outperform most individual locations in at least one of the two metrics.

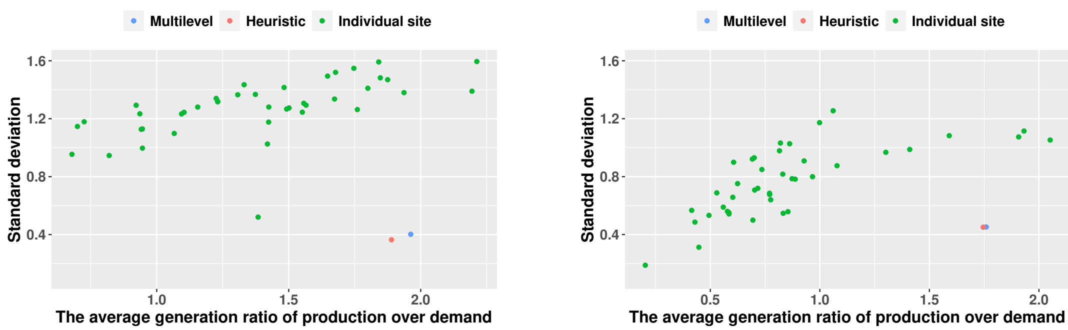

(a) Winter **(b)** Summer

Figure 4.6: Average generation and standard deviation by portfolio.

4.5.2 Effect of geographical pooling in smart grid system

The next set of experiments focuses on estimating how the different sizes of RES harvesting regions affect the improvement of operation planning in multilevel modeling. Note that smaller regions should generally correspond to more correlated outputs, and hence tend to have less potential for effective pooling [11]. We specifically investigate whether this trend is observed in the multilevel model when we move from quarter (roughly county-level) to large (state-wide) pooling. The relevant results are summarized in Fig 4.7 and Tables 4.7.

First, similarly to Figure 4.6 above, in Figure 4.7 the observed average generation ratio of production satisfy the demand, and the standard deviation is smaller than individual wind sites in all regions. At the same time, in all tested seasons, it can be observed that a larger harvesting region directly leads to a lower standard deviation. As a result, the whole pooling case (denoted as a purple dot) can be expected to be less prone to suffer from the negative effects of generation variability.

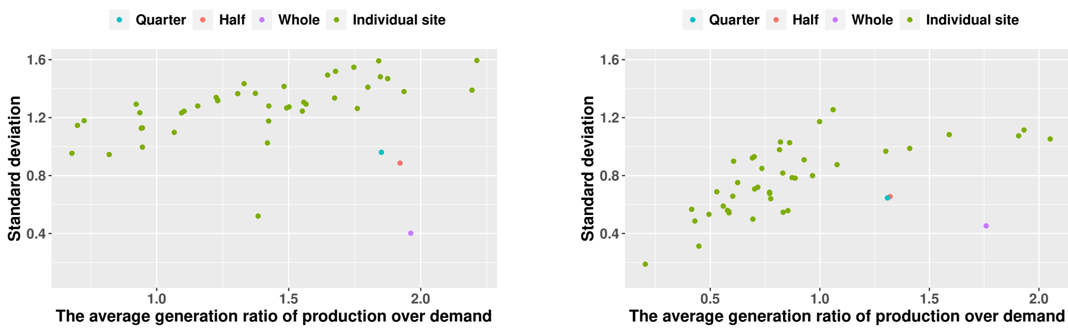

(a) Winter **(b)** Summer

Figure 4.7: Average generation and standard deviation of optimal portfolios by geographical region.

Table 4.7 reports specific optimal operation results through the different optimal pooling regions. Most importantly, it is observed that the total cost is significantly reduced as the pooling region is increased. For example, winter whole pooling (denoted as Win-W) reduces the total cost by up to 10 times ($ 60,744) compared to half pooling (denoted as Win-H) region scenario.

Scenario	Total cost ($)	Reserve cost ($)	Selling revenue ($)	Total charge energy (Kw)
Win-Q	22,611	116,309	93,695	6,556
Win-H	- 6,525	93,051	99,576	6,689
Win-W	- 67,269	30,993	98,262	7,088
Sum-Q	264,726	314,997	50,271	5,627
Sum-H	263,420	314,802	51,382	5,491
Sum-W	51,623	147,388	95,765	6,244

Table 4.7: Results of optimal portfolio performance by geographical region.

4.5.3 Sensitivity analysis

We performed a sensitivity analysis by changing battery capacity, risk tolerance parameter, and reserve energy cost.

Effect of battery capacity To investigate the effect of the battery capacity on pooling by the region, we have increased battery capacity from 9.9kw to 66kw. Table 4.8 reports the capacity of the battery modules and total cost, reserve cost, and charge energy.

Naturally, the results show that increasing battery capacity can reduce the total cost in the system when pooled across a quarter, half, and whole scenarios. Further, the reserve cost is decreased as the battery capacity is increased. At the same time, charge energy is increased as the battery capacity is increased. Note that in all cases relative performance of the harvesting regions does not change indicating that the conclusions made earlier are not sensitive to battery capacity.

Effect of risk tolerance To evaluate the effect of risk tolerance, we change parameter α from 0.2 to 0.99. $\alpha = 0.99$ corresponds to very low risk tolerance, while lower values of α represent more risk-neutral preference. Naturally, lower α allows for less focus on intermittency, and hence should result in higher generation on average. Table 4.9 and Figure 4.8 summarize the effect of risk tolerance. Table 4.9 shows that average generation (and hence amount sold on the market) are consistent with the interpretation above.

At the same time, the outcomes of the Figure 4.8 serve to highlight the important role that decreased risk tolerance plays in reducing intermittency. Both very high and very low risk tolerance can result in higher total cost, since the former restricts average generation, while the latter allows for too much intermittency.

Battery capacity(Kw)	Scenario	Total cost($)	Reserve cost($)	Charge energy(Kw)
9.9	Win-Q	22,730	116,424	3,934
	Win-H	-6,431	93,139	4,013
	Win-W	-67,210	31,042	4,227
	Sum-Q	264,913	315,189	3,344
	Sum-H	263,590	314,974	3,301
	Sum-W	51,719	147,481	3,734
16.5	Win-Q	22,611	116,309	6,556
	Win-H	-6,525	93,051	6,689
	Win-W	-67,269	30,993	7,088
	Sum-Q	264,726	314,997	5,627
	Sum-H	263,420	314,802	5,491
	Sum-W	51,623	147,388	6,244
33	Win-Q	22,321	116,026	13,087
	Win-H	-6,760	92,833	13,387
	Win-W	-67,405	30,882	14,146
	Sum-Q	264,276	314,537	11,254
	Sum-H	262,985	314,357	11,056
	Sum-W	51,388	147,164	12,479
49.5	Win-Q	22,032	115,747	19,609
	Win-H	-6,988	92,632	20,031
	Win-W	-67,541	30,777	21,172
	Sum-Q	263,829	314,080	16,917
	Sum-H	262,553	313,915	16,613
	Sum-W	51,156	146,943	18,732
66	Win-Q	21,748	115,473	26,117
	Win-H	-7,211	92,462	26,696
	Win-W	-67,675	30,662	28,266
	Sum-Q	263,388	313,630	22,503
	Sum-H	262,131	313,484	22,154
	Sum-W	50,928	146,726	24,951

Table 4.8: Results of sensitivity analysis with respect to battery capacity.

Effect of reserve energy cost To assess the effect of reserve energy cost, we have increased it from 19.15 cents to 145.45 cents. Figure 4.9 depicts total cost changes by different reserve energy unit costs.

The total cost naturally increases as the unit reserve cost is increased in all cases. However, it is important to note that the total cost of the quarter case has a more shapely increase than half and

Scenario	Risk tolerance (α)	Average wind generation(Mw/h)	Selling revenue ($)
Win-W	0.2	8,292	128,893
	0.3	8,144	123,098
	0.5	7,835	113,260
	0.7	7,628	106,889
	0.9	7,328	98,262
	0.99	6,733	82,915
Sum-W	0.2	9,106	133,388
	0.3	9,066	131,376
	0.5	8,888	124,312
	0.7	8,858	123,427
	0.9	7,864	95,765
	0.99	6,077	49,122

Table 4.9: Results of sensitivity analysis with respect to risk tolerance (generation profile).

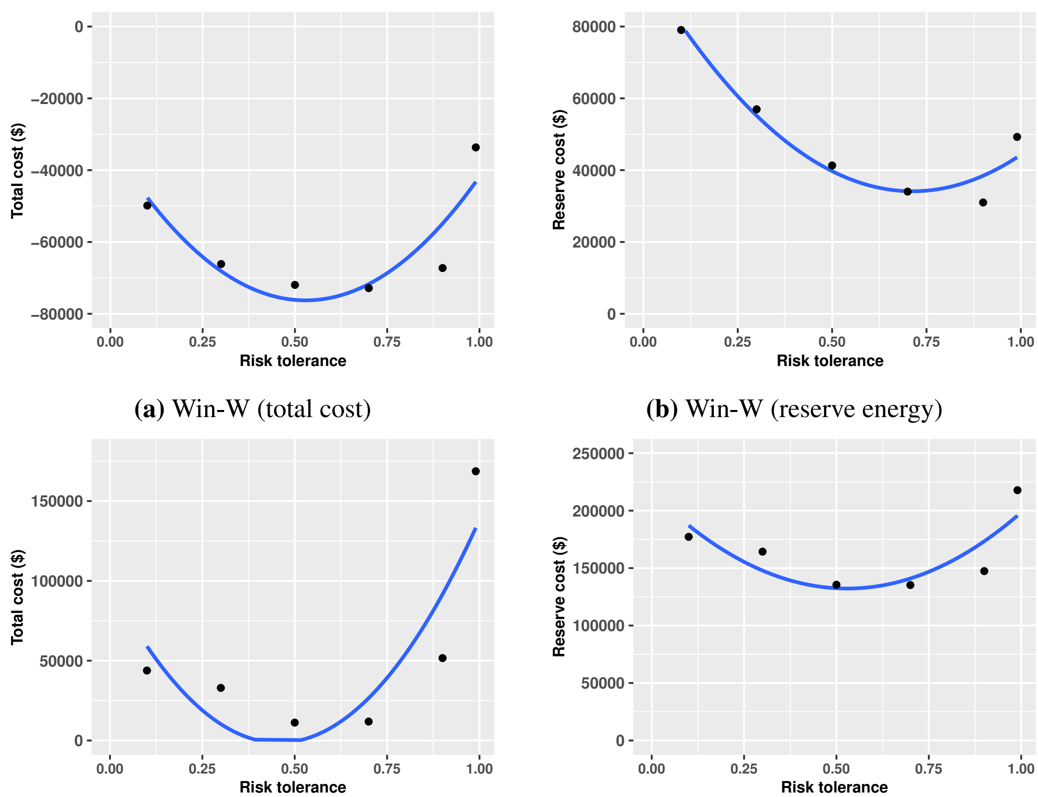

(a) Win-W (total cost)

(b) Win-W (reserve energy)

(c) Sum-W (total cost)

(d) Sum-W (reserve energy)

Figure 4.8: Results of sensitivity analysis with respect to risk tolerance (total cost).

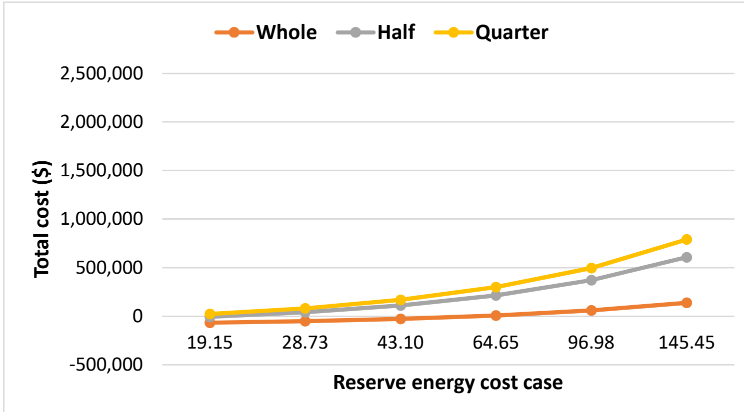

(a) Winter

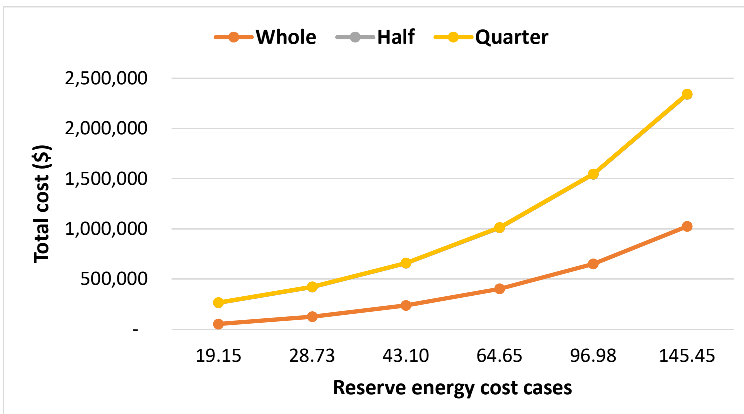

(b) Summer

Figure 4.9: Results of sensitivity analysis with respect to reserve energy cost.

whole cases, i.e., less diverse portfolios are more prone to the negative effect of reserve energy cost increase.

4.6 Conclusion

The study proposes a multilevel modeling with a risk-averse model aimed at optimizing operation planning in a virtual power plant. Specifically, on the first level, a mean-CVaR optimization model provides a family of optimal generation portfolios that achieves low intermittency based on historical forecast generation data. On the second level, the operation planning model optimizes the scheduling which consists of distributed energy sources such as wind energy and battery energy. Finally, we evaluate the performance of multilevel modeling in different scenarios such as geographically diverse wind generation locations.

Most importantly, the results have shown that multilevel model results in smaller total cost than the benchmark (heuristic methodology) in all cases. Furthermore, the outcomes of the effect of geographical pooling serve to highlight the important role that advanced pooling technique may play in VPPs design. It is observed that the total cost is significantly reduced as the pooling region is increased. It is explained by fact that a larger harvesting region (whole) directly leads to lower intermittency in the generation profile. At the same time, the total cost of the quarter case has a more shapely increase than half and whole cases as the reserve energy cost are increased or battery capacity is decreased. Consequently, the proposed model illustrates that with a multilevel modeling problem it is possible to save a total cost while managing the intermittency of generation profile at the same time.

A number of limitations and directions for future research of the study must be emphasized. First, the current study used day-ahead forecast generation data. It can be extended as a real-time dispatch tool to efficiently address distributed energy sources and load consumption uncertainty in future work. Next, research on the multilevel model effect on cost with various dispatchable energy sources such as a dispatchable battery, solar, a diesel generator is also needed. Finally, the incorporation of transmission constraints into the proposed strategy will be the focus of our future research to improve geographical pooling.

Chapter 5

Conclusions

The dissertation aims to propose optimization modeling approaches for optimal pooling of renewable energy sources through risk-averse portfolio methods. In the first stage, a portfolio optimization model for intelligently constructing a wind energy portfolio for a given harvesting region with the goal of reducing prediction error is proposed. The results showed that pooling can significantly reduce wind energy generation forecasting error, with the effect largely dependent on the size of the harvesting region. Pooling can substantially reduce the forecasting error of wind energy generation, up to 50% when pooled across a whole state compared to no pooling. On average, a 100km increase in area diameter results in a 1%–4% of reduction in average relative forecasting error, depending on the region studied. Further, if advanced optimization techniques are used, it is possible to balance this reduction with average generation output. Consequently, the results indicate that pooling has direct benefits for the renewable (wind) generation. In the remainder of the dissertation we evaluate whether these theoretical benefits can translate to cost reduction (or increase in efficiency) in a more practical setting.

The second research effort evaluates the effect of pooling on battery requirement for a residential microgrid. We proposed a two stage model with a corresponding heuristic solution approach to building a renewable energy portfolio, such that is optimizes operational cost and generation variability. The results of numerical experiments showed that the heuristic approach with pooling significantly reduces battery capacity required according to operation plans, and the effect varies on the size of the harvest region and technology used (on-shore vs off-shore). For instance, polling across both CA and WY and off-shore locations reduces the number of battery modules requested by 73% with a similar reductiin in total operational cost. In the sensitivity analysis, we can observe that pooling significantly reduces the battery requirement and the total cost in all tested scenarios, including different levels of battery cost and demand as well as grid-connected or grid-disconnected cases. Consequently, we conclude that the proposed two stage model can reduce both the overall cost of the system and battery cost through the optimal portfolio model. Intelligent planning for pooling geographically diverse renewable energy sources can serve as an important tool for overcoming generation variability challenges.

In the final chapter, we again consider simultaneous optimization of portfolio generation profile and operational costs as a bi-level problem (this time with a virtual power plant as the intended use case). We then propose an exact solution approach based on KKT conditions. We then performed a comparison of the exact and heuristic solutions in a case study, demonstrating that the proposed exact solution is able to significantly reduce the operational costs by tailoring the generation profile to the intended demand pattern.

A number of directions for future research of the study must be emphasized. First, research on the pooling effect of various renewable energy sources such as solar power is also needed. Secondly, the current study disregards transmission constraints. Both transmission cost (energy loss in transit) as well as network congestion effects have potential to reduce the extent to which the befits due to pooling can be realized in practice. Consequently, a study considering these factors is needed. Similarly, a study that considers a more practical setting for the economic analysis, including various renewable energy investment realities and considerations could further expand on practical significance of the effect of pooling that has been established in the dissertation. While we pose that the benefits due to pooling should be considered in renewable energy capital planning, a more through review of all relevant costs is required.

Appendix A

Chapter 2

A.1 Model formulation for battery sizing problem

We assume that the microgrid system is composed of a battery, external grid, and residential buildings consuming energy. The problem is constructed by directly following [58, 59, 61]. Optimization problem formulation is given below, followed by a summary of nomenclature. Parameter values used are listed in Table A.1.

Parameter	Value	Description
$P_{i,t}^{grid}$	19.15cent	Average purchasing price
S^{price}	1.3cent	Average wholesale price
AEC^{bat}	59.30 (USD)	Annual Equivalent Cost (AEC) of single battery module
$Capa^{bat}$	3.3 (kwh)	Capacity of single battery module
SOC^{min}	5%	Minimum state of charge
SOC^{max}	95%	Maximum state of charge
chr^{rate}	99%	Charging efficiency
$dchr^{rate}$	0.139%	Self-discharging efficiency
$capa^{chr}$	51%	Maximum charging power
$capa^{dchr}$	51%	Maximum discharging power
IOC	30%	Initial State Of Charge of the battery

Table A.1: Parameter values

$$\min_{x_{bat},E^{grid}_{i,t}} \quad AEC^{bat}x_{bat} + \sum_{i=1}^{I}\sum_{t=1}^{T} E^{grid}_{i,t}P^{grid}_{i,t} - \sum_{t=1}^{T} E^{sell}_{i,t}S^{price} \tag{A.1}$$

$$E^{total}_t = \sum_{i=1}^{I} E^{rew}_{i,t} + E^{chr}_t + E^{sell}_t \tag{A.2}$$

$$D^{house}_{i,t} = (E^{rew}_{i,t} + E^{dchr}_{i,t})INV^{rate} + E^{grid}_{i,t} \tag{A.3}$$

$$E^{bat}_t = E^{bat}_{t-1}(1 - dchr^{rate}) + E^{chr}_t chr^{rate} - \sum_{i=1}^{I} E^{dchr}_{i,t} \tag{A.4}$$

$$SOC^{min}C^{bat}x_{bat} \leq E^{bat}_t \leq SOC^{max}C^{bat}x_{bat} \tag{A.5}$$

$$y^{chr}_t + y^{dchr}_t \leq 1 \tag{A.6}$$

$$E^{chr}_t \leq capa^{chr}y^{chr}_t \tag{A.7}$$

$$\sum_{t=1}^{T} E^{dchr}_{i,t} \leq capa^{dchr}y^{dchr}_t \tag{A.8}$$

$$x_{bat}, E^{grid}_{i,t}, E^{sell}_{i,t}, E^{rew}_{i,t}, E^{chr}_t, E^{dchr}_{i,t}, E^{bat}_t \geq 0 \quad \forall i,t \tag{A.9}$$

$$y^{chr}_t, y^{dchr}_t \in 0,1 \quad \forall t \tag{A.10}$$

Equation (A.1) defines the objective, which is to minimize the total cost of battery and exchange with the external grid. Equation (A.2) balances the energy generation, storage and purchase/sale. Equation (A.3) guarantees that the energy demand is satisfied. In equations (A.4)–(A.8) the battery operational constraints are defined. Equations (A.4) and (A.5) describe the state of charge of the battery. Equations (A.6)–(A.8) impose limits on battery charging and discharging.

Nomenclature

Indices

i house ($i = 1 \dots I$)

t time ($t = 1 \dots T$)

Parameters

AEC^{bat} annual equivalent cost of battery (cent)

C^{bat} capacity of single battery module (kwh)

$capa^{chr}$ maximum charging power (%)

$capa^{dchr}$ maximum discharging power (%)

chr^{rate} charging efficiency (%)

$D_{i,j}^{house}$ energy consumption in house i during period t (kwh)

$dchr^{rate}$ self-discharging efficiency (%)

E_t^{total} wind energy output during period t (kwh)

INV^{rate} invereter efficiency (%)

IOC initial SOC in the battery (%)

$P_{i,t}^{grid}$ grid cost for house i during period t (cent)

S^{price} wholesale wind energy price (cent)

SOC^{max} Maximum state of charge(%)

SOC^{min} Minimum state of charge(%)

Variables

x_{bat} integer variable to indicate the number of the batteries

$E_{i,t}^{grid}$ used grid energy in house i during period t (kwh)

E_t^{sell} energy sold during period t (kwh)

$E_{i,t}^{rew}$ energy used in house i during period t (kwh)

E_t^{chr} charge energy in the battery during period t (kwh)

$E_{i,t}^{dchr}$ discharge energy in the battery to house i during period t (kwh)

E_t^{bat} available energy in the battery during period t (kwh)

y_t^{chr} binary variable indicating charging state during period t

y_t^{dchr} binary variable indicating discharging state during period t

A.2 Supplementary tables for the case study discussion

State	Year	Case	Average	Min	Max	State	Year	Case	Average	Min	Max
Alabama	2009	No-pooling	0.38	0.30	0.44	Oklahoma	2009	No-pooling	0.32	0.28	0.39
		W-CVaR	0.24	0.20	0.29			W-CVaR	0.19	0.17	0.24
		W-CVaR($\gamma = 0.9$)	0.21	0.21	0.22			W-CVaR($\gamma = 0.9$)	0.17	0.17	0.18
		Equal weight		0.22				Equal weight		0.18	
	2010	No-pooling	0.41	0.33	0.47		2010	No-pooling	0.31	0.27	0.38
		W-CVaR	0.25	0.22	0.31			W-CVaR	0.18	0.16	0.24
		W-CVaR($\gamma = 0.9$)	0.24	0.23	0.24			W-CVaR($\gamma = 0.9$)	0.17	0.17	0.17
		Equal weight		0.24				Equal weight		0.18	
	2011	No-pooling	0.39	0.30	0.46		2011	No-pooling	0.30	0.26	0.39
		W-CVaR	0.24	0.21	0.28			W-CVaR	0.18	0.16	0.24
		W-CVaR($\gamma = 0.9$)	0.22	0.22	0.22			W-CVaR($\gamma = 0.9$)	0.17	0.16	0.17
		Equal weight		0.24				Equal weight		0.17	
	2012	No-pooling	0.42	0.32	0.49		2012	No-pooling	0.32	0.27	0.37
		W-CVaR	0.26	0.22	0.31			W-CVaR	0.19	0.17	0.24
		W-CVaR($\gamma = 0.9$)	0.23	0.23	0.24			W-CVaR($\gamma = 0.9$)	0.18	0.17	0.18
		Equal weight		0.25				Equal weight		0.18	
Arizona	2009	No-pooling	0.53	0.32	0.71	South Dakota	2009	No-pooling	0.35	0.28	0.60
		W-CVaR	0.22	0.18	0.30			W-CVaR	0.21	0.18	0.39
		W-CVaR($\gamma = 0.9$)	0.21	0.20	0.21			W-CVaR($\gamma = 0.9$)	0.19	0.19	0.19
		Equal weight		0.21				Equal weight		0.21	
	2010	No-pooling	0.50	0.27	0.70		2010	No-pooling	0.35	0.29	0.61
		W-CVaR	0.19	0.16	0.28			W-CVaR	0.22	0.19	0.38
		W-CVaR($\gamma = 0.9$)	0.18	0.18	0.19			W-CVaR($\gamma = 0.9$)	0.19	0.19	0.20
		Equal weight		0.19				Equal weight		0.21	
	2011	No-pooling	0.51	0.29	0.70		2011	No-pooling	0.35	0.28	0.56
		W-CVaR	0.21	0.17	0.30			W-CVaR	0.21	0.18	0.38
		W-CVaR($\gamma = 0.9$)	0.20	0.19	0.20			W-CVaR($\gamma = 0.9$)	0.19	0.19	0.19
		Equal weight		0.20				Equal weight		0.21	
	2012	No-pooling	0.55	0.32	0.76		2012	No-pooling	0.36	0.29	0.57
		W-CVaR	0.22	0.18	0.30			W-CVaR	0.21	0.18	0.38
		W-CVaR($\gamma = 0.9$)	0.21	0.21	0.22			W-CVaR($\gamma = 0.9$)	0.19	0.18	0.19
		Equal weight		0.22				Equal weight		0.21	
Ohio	2009	No-pooling	0.33	0.30	0.41	Washington	2009	No-pooling	0.52	0.30	1.18
		W-CVaR	0.22	0.20	0.25			W-CVaR	0.20	0.15	0.29
		W-CVaR($\gamma = 0.9$)	0.21	0.21	0.21			W-CVaR($\gamma = 0.9$)	0.23	0.22	0.23
		Equal weight		0.22				Equal weight		0.20	
	2010	No-pooling	0.35	0.30	0.43		2010	No-pooling	0.49	0.28	1.13
		W-CVaR	0.22	0.21	0.26			W-CVaR	0.17	0.13	0.21
		W-CVaR($\gamma = 0.9$)	0.21	0.21	0.22			W-CVaR($\gamma = 0.9$)	0.21	0.21	0.21
		Equal weight		0.22				Equal weight		0.17	
	2011	No-pooling	0.34	0.31	0.41		2011	No-pooling	0.49	0.30	0.97
		W-CVaR	0.21	0.20	0.25			W-CVaR	0.19	0.14	0.30
		W-CVaR($\gamma = 0.9$)	0.20	0.20	0.21			W-CVaR($\gamma = 0.9$)	0.22	0.22	0.22
		Equal weight		0.21				Equal weight		0.18	
	2012	No-pooling	0.34	0.31	0.42		2012	No-pooling	0.49	0.30	1.00
		W-CVaR	0.22	0.21	0.26			W-CVaR	0.19	0.14	0.28
		W-CVaR($\gamma = 0.9$)	0.22	0.21	0.22			W-CVaR($\gamma = 0.9$)	0.21	0.20	0.21
		Equal weight		0.23				Equal weight		0.18	

Table A.2: Obtained forecasting error (δ) in the considered portfolios (no pooling, optimal pooling, optimal pooling at 90% of max generation and equal weight) for state-wide pooling cases.

State	Year	Region	Average	Min	Max	Year	Region	Average	Min	Max	Year	Region	Average	Min	Max	Year	Region	Average	Min	Max
		small	0.33	0.29	0.35		small	0.34	0.31	0.35		small	0.33	0.31	0.35		small	0.36	0.32	0.38
		medium	0.29	0.26	0.32		medium	0.30	0.28	0.34		medium	0.30	0.27	0.34		medium	0.32	0.28	0.35
Alabama	2009	quarter	0.27	0.25	0.32	2010	quarter	0.29	0.26	0.33	2011	quarter	0.28	0.25	0.32	2012	quarter	0.30	0.27	0.36
		half	0.25	0.23	0.29		half	0.27	0.25	0.30		half	0.26	0.24	0.29		half	0.28	0.25	0.32
		whole	0.23	0.21	0.25		whole	0.25	0.23	0.26		whole	0.24	0.22	0.25		whole	0.25	0.23	0.27
		small	0.40	0.32	0.66		small	0.36	0.28	0.64		small	0.36	0.29	0.60		small	0.39	0.32	0.63
		medium	0.39	0.33	0.66		medium	0.36	0.29	0.64		medium	0.37	0.31	0.60		medium	0.39	0.33	0.63
Arizona	2009	quarter	0.33	0.23	0.57	2010	quarter	0.31	0.20	0.55	2011	quarter	0.32	0.22	0.52	2012	quarter	0.34	0.23	0.55
		half	0.29	0.21	0.46		half	0.27	0.19	0.44		half	0.28	0.20	0.43		half	0.29	0.21	0.45
		whole	0.23	0.18	0.30		whole	0.21	0.16	0.28		whole	0.22	0.17	0.30		whole	0.23	0.18	0.30
		small	0.26	0.24	0.30		small	0.27	0.24	0.32		small	0.26	0.24	0.30		small	0.27	0.24	0.31
		medium	0.26	0.23	0.31		medium	0.27	0.23	0.31		medium	0.26	0.22	0.31		medium	0.27	0.23	0.32
Ohio	2009	quarter	0.24	0.23	0.29	2010	quarter	0.25	0.23	0.31	2011	quarter	0.24	0.22	0.30	2012	quarter	0.25	0.23	0.31
		half	0.24	0.21	0.26		half	0.24	0.21	0.27		half	0.23	0.21	0.26		half	0.24	0.22	0.27
		whole	0.22	0.20	0.24		whole	0.22	0.21	0.24		whole	0.21	0.20	0.24		whole	0.22	0.21	0.25
		small	0.25	0.24	0.31		small	0.25	0.23	0.31		small	0.24	0.22	0.30		small	0.26	0.23	0.31
		medium	0.25	0.21	0.32		medium	0.25	0.21	0.31		medium	0.23	0.20	0.30		medium	0.25	0.21	0.33
Oklahoma	2009	quarter	0.24	0.19	0.32	2010	quarter	0.23	0.19	0.31	2011	quarter	0.22	0.18	0.30	2012	quarter	0.24	0.19	0.33
		half	0.23	0.18	0.32		half	0.22	0.17	0.31		half	0.21	0.17	0.28		half	0.23	0.17	0.33
		whole	0.19	0.17	0.24		whole	0.19	0.16	0.24		whole	0.18	0.16	0.22		whole	0.19	0.17	0.24
		small	0.28	0.27	0.31		small	0.28	0.27	0.32		small	0.28	0.27	0.32		small	0.28	0.26	0.30
		medium	0.25	0.23	0.28		medium	0.25	0.23	0.28		medium	0.26	0.24	0.29		medium	0.25	0.23	0.27
South Dakota	2009	quarter	0.24	0.21	0.40	2010	quarter	0.24	0.22	0.40	2011	quarter	0.24	0.21	0.40	2012	quarter	0.23	0.21	0.40
		half	0.24	0.20	0.40		half	0.24	0.21	0.40		half	0.24	0.21	0.40		half	0.24	0.20	0.40
		whole	0.24	0.19	0.39		whole	0.24	0.19	0.38		whole	0.24	0.19	0.38		whole	0.24	0.18	0.38
		small	0.40	0.31	0.52		small	0.40	0.32	0.55		small	0.36	0.29	0.44		small	0.36	0.30	0.47
		medium	0.30	0.25	0.34		medium	0.29	0.24	0.34		medium	0.28	0.23	0.31		medium	0.28	0.23	0.33
Washington	2009	quarter	0.24	0.21	0.30	2010	quarter	0.22	0.18	0.28	2011	quarter	0.22	0.19	0.28	2012	quarter	0.22	0.19	0.28
		half	0.21	0.18	0.26		half	0.19	0.16	0.24		half	0.20	0.16	0.24		half	0.19	0.16	0.24
		whole	0.19	0.15	0.23		whole	0.17	0.13	0.21		whole	0.18	0.14	0.22		whole	0.17	0.14	0.21

Table A.3: Effect of harvesting region size on the achieved forecasting error. Relative error δ is reported for all testing states, subareas and years.

Appendix B

Chapter 4

B.1 Supplementary tables for the case study discussion

	Winter			Summer		
Wind site	Hueristic	Multilevel	Absolute difference	Hueristic	Multilevel	Absolute different
1	14.05%	15.27%	1.22%	0.00%	0.00%	0.00%
2	3.83%	4.48%	0.65%	25.56%	26.03%	0.47%
3	21.30%	29.42%	8.12%	0.00%	0.00%	0.00%
4	0.00%	0.00%	0.00%	0.00%	0.00%	0.00%
5	0.00%	0.00%	0.00%	0.00%	0.00%	0.00%
6	0.00%	0.00%	0.00%	0.00%	0.00%	0.00%
7	9.42%	0.00%	9.42%	0.00%	0.00%	0.00%
8	0.00%	0.00%	0.00%	7.34%	6.54%	0.80%
9	0.00%	0.00%	0.00%	0.00%	0.00%	0.00%
10	0.00%	0.00%	0.00%	0.00%	0.00%	0.00%
11	0.00%	0.00%	0.00%	0.00%	0.00%	0.00%
12	0.00%	0.00%	0.00%	0.00%	0.00%	0.00%
13	0.00%	0.00%	0.00%	0.00%	0.00%	0.00%
14	0.00%	0.00%	0.00%	0.00%	0.00%	0.00%
15	23.69%	22.99%	0.71%	0.00%	0.00%	0.00%
16	0.00%	0.00%	0.00%	0.00%	0.00%	0.00%
17	0.00%	0.00%	0.00%	0.00%	0.00%	0.00%
18	0.00%	0.00%	0.00%	0.00%	0.00%	0.00%
19	0.00%	0.00%	0.00%	0.00%	0.00%	0.00%
20	0.00%	0.00%	0.00%	0.00%	0.00%	0.00%
21	0.00%	0.00%	0.00%	54.57%	55.16%	0.58%
22	0.00%	0.00%	0.00%	0.00%	0.00%	0.00%
23	0.00%	0.00%	0.00%	0.00%	0.00%	0.00%
24	0.00%	0.00%	0.00%	5.03%	5.07%	0.03%
25	0.00%	0.00%	0.00%	0.00%	0.00%	0.00%
26	0.00%	0.00%	0.00%	0.00%	0.00%	0.00%
27	0.00%	0.00%	0.00%	0.00%	0.00%	0.00%
28	0.00%	0.00%	0.00%	0.24%	0.30%	0.06%
29	0.00%	0.00%	0.00%	0.00%	0.00%	0.00%
30	0.00%	0.00%	0.00%	0.00%	0.00%	0.00%
31	0.00%	0.00%	0.00%	0.00%	0.00%	0.00%
32	0.00%	0.00%	0.00%	0.00%	0.00%	0.00%
33	0.00%	2.99%	2.99%	0.00%	0.00%	0.00%
34	7.98%	9.90%	1.92%	4.19%	4.31%	0.12%
35	9.07%	11.18%	2.11%	0.79%	0.55%	0.24%
36	0.00%	0.00%	0.00%	0.00%	0.00%	0.00%
37	0.00%	0.00%	0.00%	0.00%	0.00%	0.00%
38	8.31%	3.38%	4.92%	0.00%	0.00%	0.00%
39	2.35%	0.38%	1.97%	2.27%	2.05%	0.22%
40	0.00%	0.00%	0.00%	0.00%	0.00%	0.00%
	Total absolute difference of investment level		34.04%	Total absolute difference of investment level		2.52%

Table B.1: Comparison of the two optimal portfolios.

References

[1] J. Zhang, B.-M. Hodge, A. Florita, Investigating the correlation between wind and solar power forecast errors in the western interconnection, American Society of Mechanical Engineers Digital Collection. (2013). doi:10.1115/ES2013-18423.

[2] G. Ren, J. Liu, J. Wan, Y. Guo, D. Yu, J. Liu, Measurement and statistical analysis of wind speed intermittency, Energy 118 (2017) 632–643. doi:10.1016/j.energy.2016.10.096.

[3] T. Barbounis, J. Theocharis, M. Alexiadis, P. Dokopoulos, Long-term wind speed and power forecasting using local recurrent neural network models, IEEE Transactions on Energy Conversion 21 (1) (2006) 273–284. doi:10.1109/TEC.2005.847954.

[4] GWEC, Global wind 2008 technical report, `https://gwec.net/wp-content/uploads/2012/06/Global-Wind-2008-Report.pdf` (2009).

[5] C. Chen, S. Duan, T. Cai, B. Liu, Online 24-h solar power forecasting based on weather type classification using artificial neural network, Solar Energy 85 (11) (2011) 2856–2870. doi:10.1016/j.solener.2011.08.027.

[6] T. W. EXPRESSLLC.

[7] M. Rekik, Z. Chtourou, N. Mitton, A. Atieh, Geographic routing protocol for the deployment of virtual power plant within the smart grid, Sustainable Cities and Society 25 (2016) 39–48. doi:10.1016/j.scs.2015.12.003.

[8] B. Moreno, G. Díaz, The impact of virtual power plant technology composition on wholesale electricity prices: A comparative study of some european union electricity markets, Renewable and Sustainable Energy Reviews 99 (2019) 100–108. doi:10.1016/j.rser.2018.09.028.

[9] B. Hrnvcić, A. Pfeifer, F. Jurić, N. Duić, V. Ivanović, I. Vuvsanović, Different investment dynamics in energy transition towards a 100% renewable energy system, Energy 237 (2021) 121526. doi:10.1016/j.energy.2021.121526.

[10] international tertiary education research database, Communication from the commission to the european parliament, the council, the european economic and social committee and the committee of the regions: Youth opportunities initiative, https://www.voced.edu.au/content/.

[11] C. Han, A. Vinel, Reducing forecasting error by optimally pooling wind energy generation sources through portfolio optimization, Energy 239 (2022) 122099. doi:10.1016/j.energy.2021.122099.

[12] J. Huang, X. Lu, M. B. McElroy, Meteorologically defined limits to reduction in the variability of outputs from a coupled wind farm system in the central US, Renewable Energy 62 (2014) 331–340. doi:10.1016/j.renene.2013.07.022.

[13] M. Grubb, D. Newbery, UK electricity market reform and the energy transition: Emerging lessons, The Energy Journal 39 (1) (2018). doi:10.5547/01956574.39.6.mgru.

[14] R. Lahon, C. P. Gupta, Risk-based coalition of cooperative microgrids in electricity market environment, IET Generation, Transmission & Distribution 12 (13) (2018) 3230–3241. doi:10.1049/iet-gtd.2017.1562.

[15] A. Vinel, E. Mortaz, Optimal pooling of renewable energy sources with a risk-averse approach: Implications for US energy portfolio, Energy Policy 132 (2019) 928–939. doi:10.1016/j.enpol.2019.06.051.

[16] J. Widén, Correlations between large-scale solar and wind power in a future scenario for sweden, IEEE transactions on sustainable energy 2 (2) (2011) 177–184. doi:10.1109/TSTE.2010.2101620.

[17] F. Santos-Alamillos, D. Pozo-Vázquez, J. Ruiz-Arias, V. Lara-Fanego, J. Tovar-Pescador, Analysis of spatiotemporal balancing between wind and solar energy resources in the southern iberian peninsula, Journal of Applied Meteorology and Climatology 51 (11) (2012) 2005–2024. doi:10.1175/JAMC-D-11-0189.1.

[18] P. E. Bett, H. E. Thornton, The climatological relationships between wind and solar energy supply in britain, Renewable Energy 87 (2016) 96–110. doi:10.1016/j.renene.2015.10.006.

[19] M. Shahriari, S. Blumsack, Scaling of wind energy variability over space and time, Applied Energy 195 (2017) 572–585. doi:10.1016/j.apenergy.2017.03.073.

[20] M. A. Handschy, S. Rose, J. Apt, Is it always windy somewhere? occurrence of low-wind-power events over large areas, Renewable Energy 101 (2017) 1124–1130. doi:10.1016/j.renene.2016.10.004.

[21] W. Katzenstein, E. Fertig, J. Apt, The variability of interconnected wind plants, Energy Policy 38 (8) (2010) 4400–4410. doi:10.1016/j.enpol.2010.03.069.

[22] B. Sun, Risk-averse design and operation of renewable energy power grids, The University of Iowa, 2015. doi:10.17077/etd.n9d4ouj6.

[23] R. Mena, M. Hennebel, Y.-F. Li, C. Ruiz, E. Zio, A risk-based simulation and multi-objective optimization framework for the integration of distributed renewable generation and storage, Renewable and Sustainable Energy Reviews 37 (2014) 778–793. doi:10.1016/j.rser.2014.05.046.

[24] G. Gersema, D. Wozabal, Risk-optimized pooling of intermittent renewable energy sources, Journal of Banking & Finance 95 (2018) 217–230. doi:10.1016/j.jbankfin.2017.03.016.

[25] J. I. Munoz, A. A. S. de la Nieta, J. Contreras, J. L. Bernal-Agustín, Corrigendum to "optimal investment portfolio in renewable energy: The spanish case" [energy policy 37 (2009) 5273–5284], Energy Policy 38 (5) (2010) 2608. doi:10.1016/j.enpol.2009.11.051.

[26] T. K. Boomsma, N. Meade, S.-E. Fleten, Renewable energy investments under different support schemes: A real options approach, European Journal of Operational Research 220 (1) (2012) 225–237. doi:10.1016/j.ejor.2012.01.017.

[27] M. Shahriari, S. Blumsack, The capacity value of optimal wind and solar portfolios, Energy 148 (2018) 992–1005. doi:10.1016/j.energy.2017.12.121.

[28] J. Apt, P. Jaramillo, Variable Renewable Energy and the Electricity Grid, 1st Edition, Routledge, 2014. doi:10.4324/9781315848709.

[29] C. Sweeney, R. J. Bessa, J. Browell, P. Pinson, The future of forecasting for renewable energy, WIREs Energy and Environment 9 (2) (2020) 365. doi:https://doi.org/10.1002/wene.365.

[30] M. A. F. Lima, P. C. Carvalho, T. C. Carneiro, J. R. Leite, L. J. d. Bessa Neto, G. K. Rodrigues, F. E. d. Melo, Portfolio theory applied to solar and wind resources forecast, IET Renewable Power Generation 11 (7) (2017) 973–978. doi:10.1049/iet-rpg.2017.0006.

[31] A. M. Foley, P. G. Leahy, A. Marvuglia, E. J. McKeogh, Current methods and advances in forecasting of wind power generation, Renewable Energy 37 (1) (2012) 1–8. doi:10.1016/j.renene.2011.05.033.

[32] K. Methaprayoon, C. Yingvivatanapong, W.-J. Lee, J. R. Liao, An integration of ANN wind power estimation into unit commitment considering the forecasting uncertainty, IEEE Transactions on Industry Applications 43 (6) (2007) 1441–1448. doi:10.1109/TIA.2007.908203.

[33] J. L. Torres, A. García, M. De Blas, A. De Francisco, Forecast of hourly average wind speed with ARMA models in navarre (spain), Solar Energy 79 (1) (2005) 65–77. doi:10.1016/j.solener.2004.09.013.

[34] D. P. Larson, L. Nonnenmacher, C. F. M. Coimbra, Day-ahead forecasting of solar power output from photovoltaic plants in the american southwest, Renewable Energy 91 (2016) 11–20. doi:10.1016/j.renene.2016.01.039.

[35] NREL, Wind data, `https://doi.org/10.17041/drp/1473618`.

[36] P. A. Jiménez, J. Dudhia, Improving the representation of resolved and unresolved topographic effects on surface wind in the WRF model, Journal of Applied Meteorology and Climatology 51 (2) (2012) 300–316. doi:10.1175/JAMC-D-11-084.1.

[37] W. C. Skamarock, J. B. Klemp, J. Dudhia, D. O. Gill, D. M. Barker, W. Wang, J. G. Powers, A description of the advanced research WRF version 2 (2005).

[38] I. Mauleón, H. Hamoudi, Photovoltaic and wind cost decrease estimation: Implications for investment analysis, Energy 137 (2017) 1054–1065. doi:10.1016/j.energy.2017.03.109.

[39] I. Mauleón, Assessing PV and wind roadmaps: Learning rates, risk, and social discounting, Renewable and Sustainable Energy Reviews 100 (2019). doi:10.1016/j.rser.2018.10.012.

[40] R. T. Rockafellar, S. Uryasev, Optimization of conditional value-at-risk, The Journal of Risk 2 (3) (2000) 21–41. doi:10.21314/JOR.2000.038.

[41] R. T. Rockafellar, S. Uryasev, Conditional value-at-risk for general loss distributions, Journal of Banking & Finance 26 (7) (2002) 1443–1471. doi:10.1016/S0378-4266(02)00271-6.

[42] M. S. Nazari, B. Maybee, J. Whale, A. McHugh, Climate policy uncertainty and power generation investments: A real options-CVaR portfolio optimization approach, Energy Procedia 75 (2015) 2649–2657. doi:10.1016/j.egypro.2015.07.367.

[43] R. J. Bianchi, G. Bornholt, M. E. Drew, M. F. Howard, Long-term u.s. infrastructure returns and portfolio selection, Journal of Banking & Finance 42 (2014) 314–325. doi:10.1016/j.jbankfin.2014.01.034.

[44] C. Sahin, M. Shahidehpour, I. Erkmen, Generation risk assessment in volatile conditions with wind, hydro, and natural gas units, Applied Energy 96 (2012) 4–11. doi:10.1016/j.apenergy.2011.11.007.

[45] A. A. Sanchez de la Nieta, J. Contreras, J. I. Munoz, J. P. S. Catalao, Optimal wind reversible hydro offering strategies for midterm planning, IEEE Transactions on Sustainable Energy 6 (4) (2015) 1356–1366. doi:10.1109/TSTE.2015.2437974.

[46] J. Morales, A. Conejo, J. Perez-Ruiz, Short-term trading for a wind power producer, IEEE Transactions on Power Systems 25 (1) (2010) 554–564. doi:10.1109/TPWRS.2009.2036810.

[47] Z. Tan, G. Wang, L. Ju, Q. Tan, W. Yang, Application of CVaR risk aversion approach in the dynamical scheduling optimization model for virtual power plant connected with wind-photovoltaic-energy storage system with uncertainties and demand response, Energy 124 (2017) 198–213. doi:10.1016/j.energy.2017.02.063.

[48] N. Jovanović, J. García-González, J. Barquín, S. Cerisola, Electricity market short-term risk management via risk-adjusted probability measures, IET Generation, Transmission & Distribution 11 (10) (2017) 2599–2607. doi:10.1049/iet-gtd.2016.1731.

[49] J. C. do Prado, W. Qiao, A stochastic decision-making model for an electricity retailer with intermittent renewable energy and short-term demand response, IEEE Transactions on Smart Grid 10 (3) (2019) 2581–2592. doi:10.1109/TSG.2018.2805326.

[50] A. Papakonstantinou, G. Champeri, S. Delikaraoglou, P. Pinson, Trading wind power through physically settled options and short-term electricity markets, Wind Energy 22 (11) (2019) 1487–1499. doi:10.1002/we.2383.

[51] P. Krokhmal, M. Zabarankin, S. Uryasev, Modeling and optimization of risk, Surveys in Operations Research and Management Science 16 (2) (2011) 49–66. doi:10.1016/j.sorms.2010.08.001.

[52] C. Draxl, A. Clifton, B.-M. Hodge, J. McCaa, The wind integration national dataset (wind) toolkit, Applied Energy 151 (2015) 355–366. doi:10.1016/j.apenergy.2015.03.121.

[53] EIA, Annual energy outlook 2019, `https://www.eia.gov/outlooks/archive/aeo19/`.

[54] J. D. Rhodes, C. King, G. Gulen, S. M. Olmstead, J. S. Dyer, R. E. Hebner, F. C. Beach, T. F. Edgar, M. E. Webber, A geographically resolved method to estimate levelized power plant costs with environmental externalities, Energy Policy 102 (2017) 491–499. doi:10.1016/j.enpol.2016.12.025.

[55] J. Hernández-Moro, J. M. Martínez-Duart, Analytical model for solar PV and CSP electricity costs: Present LCOE values and their future evolution, Renewable and Sustainable Energy Reviews 20 (2013) 119–132. doi:10.1016/j.rser.2012.11.082.

[56] M. Tahanan, W. van Ackooij, A. Frangioni, F. Lacalandra, Large-scale unit commitment under uncertainty, 4OR 13 (2) (2015) 115–171. doi:10.1007/s10288-014-0279-y.

[57] IBM, www.cplex.com.

[58] M. Korpaas, A. T. Holen, R. Hildrum, Operation and sizing of energy storage for wind power plants in a market system, International Journal of Electrical Power & Energy Systems 25 (8) (2003) 599–606. doi:10.1016/S0142-0615(03)00016-4.

[59] D. Cho, J. Valenzuela, Scheduling energy consumption for residential stand-alone photovoltaic systems, Solar Energy 187 (2019) 393–403. doi:10.1016/j.solener.2019.05.054.

[60] EIA, Electric sales, revenue, and average price - energy information administration, https://www.eia.gov/electricity/sales_revenue_price/ (2020).

[61] D. Cho, J. Valenzuela, Optimization of residential off-grid PV-battery systems, Solar Energy 208 (2020) 766–777. doi:10.1016/j.solener.2020.08.023.

[62] Y. Rombauts, E. Delarue, W. D'haeseleer, Optimal portfolio-theory-based allocation of wind power: Taking into account cross-border transmission-capacity constraints, Renewable Energy 36 (9) (2011) 2374–2387. doi:10.1016/j.renene.2011.02.010.

[63] DOE, Solving challenges in energy storage - updated july 2019 u.s department of energy, https://www.energy.gov/sites/default/files/2019/07/f64/2018-OTT-Energy-Storage-Spotlight.pdf (2019).

[64] H. O. R. Howlader, H. Matayoshi, T. Senjyu, Distributed generation integrated with thermal unit commitment considering demand response for energy storage optimization of smart grid, Renewable Energy 99 (2016) 107–117. doi:10.1016/j.renene.2016.06.050.

[65] M. A. Abdulgalil, M. Khalid, Enhancing the reliability of a microgrid through optimal size of battery ESS, IET Generation, Transmission & Distribution 13 (9) (2019) 1499–1508. doi:https://doi.org/10.1049/iet-gtd.2018.5335.

[66] K. Chaudhari, A. Ukil, K. N. Kumar, U. Manandhar, S. K. Kollimalla, Hybrid optimization for economic deployment of ESS in PV-integrated EV charging stations, IEEE Transactions on Industrial Informatics 14 (1) (2018) 106–116. doi:10.1109/TII.2017.2713481.

[67] L. Bridier, M. David, P. Lauret, Optimal design of a storage system coupled with intermittent renewables, Renewable Energy 67 (2014) 2–9. doi:10.1016/j.renene.2013.11.048.

[68] C.-T. Li, H. Peng, J. Sun, Predictive control and sizing of energy storage to mitigate wind power intermittency, Wind Energy 19 (3) (2016) 437–451. doi:https://doi.org/10.1002/we.1843.

[69] M. A. Mohamed, A. M. Eltamaly, A. I. Alolah, PSO-based smart grid application for sizing and optimization of hybrid renewable energy systems, PLOS ONE 11 (8) (2016) e0159702. doi:10.1371/journal.pone.0159702.

[70] D. Cho, J. Valenzuela, Optimization of residential off-grid PV-battery systems, Solar Energy 208 (2020) 766–777. doi:10.1016/j.solener.2020.08.023.

[71] H. Qiao, Q. Wei, Functional nanofibers in lithium-ion batteries, Elsevier, 2012. doi:10.1533/9780857095640.2.197.

[72] EIA, California state grid cost, `https://www.eia.gov/electricity/gridmonitor/dashboard/electric_overview/US48/US48` (2019).

[73] A. Mills, R. Wiser, D. Millstein, J. P. Carvallo, W. Gorman, J. Seel, S. Jeong, The impact of wind, solar, and other factors on the decline in wholesale power prices in the united states, Applied Energy 283 (2021) 116266. doi:10.1016/j.apenergy.2020.116266.

[74] W. E. Hart, G. A. Hackebeil, C. D. Laird, B. L. Nicholson, J. D. Siirola, J.-P. Watson, D. L. Woodruff, Pyomo - Optimization Modeling in Python, 2nd Edition, no. 67 in Springer Optimization and Its Applications, Springer International Publishing : Imprint: Springer, 2017.

[75] W. Cole, A. Frazier, Cost projections for utility-scale battery storage: 2020 update (2020). doi:https://doi.org/10.2172/1665769.

[76] K. Zhou, S. Yang, Z. Shao, Energy internet: The business perspective, Applied Energy 178 (2016) 212–222. doi:10.1016/j.apenergy.2016.06.052.

[77] S. Yu, F. Fang, Y. Liu, J. Liu, Uncertainties of virtual power plant: Problems and countermeasures, Applied Energy 239 (2019) 454–470. doi:10.1016/j.apenergy.2019.01.224.

[78] T. Zhang, Z. Hu, Optimal scheduling strategy of virtual power plant (VPP) with power-to-gas in dual energy markets, IEEE Transactions on Industry Applications (2021) 1–1doi:10.1109/TIA.2021.3112641.

[79] S. Awerbuch, Portfolio-based electricity generation planning: Policy implications for renewables and energy security, Mitigation and Adaptation Strategies for Global Change 11 (3) (2006) 693–710. doi:10.1007/s11027-006-4754-4.

[80] N. Etherden, V. Vyatkin, M. H. J. Bollen, Virtual power plant for grid services using IEC 61850, IEEE Transactions on Industrial Informatics 12 (1) (2016) 437–447. doi:10.1109/TII.2015.2414354.

[81] M. Ortega-Vazquez, D. Kirschen, Estimating the spinning reserve requirements in systems with significant wind power generation penetration, IEEE Transactions on Power Systems 24 (1) (2009) 114–124. doi:10.1109/TPWRS.2008.2004745.

[82] W. F. Bialas, M. H. Karwan, Two-level linear programming, Management Science 30 (8) (1984) 1004–1020. doi:10.1287/mnsc.30.8.1004.

[83] L. N. Vicente, P. H. Calamai, Bilevel and multilevel programming: A bibliography review, Journal of Global Optimization 5 (3) (1994) 291–306. doi:10.1007/BF01096458.

[84] S. Boyd, S. P. Boyd, L. Vandenberghe, Convex Optimization, Cambridge University Press, 2004.

[85] W. Ogryczak, T. Śliwiński, On solving the dual for portfolio selection by optimizing conditional value at risk, Computational Optimization and Applications 50 (3) (2011) 591–595. doi:10.1007/s10589-010-9321-y.

[86] LG Energy Solution, `https://www.lgessbattery.com/m/us/main/main.lg`.

[87] P. C. Bhagwat, J. C. Richstein, E. J. Chappin, L. J. de Vries, The effectiveness of a strategic reserve in the presence of a high portfolio share of renewable energy sources, Utilities Policy 39 (2016) 13–28. doi:10.1016/j.jup.2016.01.006.